U.PORTO

MASTER
NEUROBIOLOGY

Developing a protein biotinylation system to unravel the astrocyte-specific secretome

Luísa Maria Araújo Florido

M

2024

Developing a protein biotinylation system to unravel the astrocyte-specific secretome

Luísa Maria Araújo Florido

Synapse Biology Group

Instituto de Investigação e Inovação em Saúde

Master in Neurobiology

Supervisor: Matthew Holt, PhD

Dissertação apresentada à Universidade do Porto para cumprimentos dos requisitos necessários à obtenção do grau de Mestre em Neurobiologia realizada sob a orientação científica do Doutor Matthew Holt, Group Leader do grupo Synapse Biology no i3S (Instituto de Investigação e Inovação em Saúde da Universidade do Porto), onde esta tese foi realizada.

Dissertation submitted to the University of Porto to obtain the degree of Master of Science in Neurobiology developed under the scientific supervision of Dr Matthew Holt, Group Leader of the Synapse Biology group at i3S (Instituto de Investigação e Inovação em Saúde da Universidade do Porto), where this thesis was carried out.

This project was funded by the European Union's Horizon 2020 research and innovation programme under the Grant Agreement no. 951923.

Acknowledgements

First and foremost, I would like to express my gratitude to Matthew for all the guidance and support and for always challenging me and keeping me curious about science.

I would also like to thank every member of the Synapse Biology Lab because every one of them helped me in their unique way throughout this year and made this work possible. My deepest gratitude goes to Simone for everything she did for this project, for all the guidance and patience, and for João, my Lab big brother. Thank you for every tip, every discussion, every talk, for all your patience, trust and kindness.

A very special thanks also goes to all my loved ones. To my parents, Clara and Luísa, for all the patience, love and support, and to Joaninha for all the joy. To all my friends, especially to the Borbolets, who I am very thankful I met; to Vasco, for always being there for me; and to Leonor, for all the evenings, talks and endless support. Lastly, my deepest gratitude goes to Henry for all his kindness and joy, for the immeasurable support, and for always being my safest place.

Abstract

Neurons communicate at specialist points of contact called synapses that can be excitatory or inhibitory depending on the neurotransmitter used and the effect they elicit. Correct synapse formation and maturation are essential for maintaining the excitation/inhibition balance in the brain, with aberrant synapse formation linked to a range of neurodevelopment disorders. Astrocytes are closely associated with synapses and have been shown to regulate synaptic formation and function through cell surface adhesion molecules and secreted proteins. However, many of these factors are yet to be identified, especially those involved in inhibitory synapse assembly and maturation.

I aim to develop a system that will allow the host group to identify astrocyte-secreted factors that could be involved in inhibitory or excitatory synapse formation. To do this, TurboID, a promiscuous biotin ligase, can be directed to the ER of primary astrocytes to biotinylate proteins that will then be secreted into the medium. After an easy one-step purification, rather than the labour-intensive chromatographic approaches used to date, biotinylated proteins in the medium can be identified by mass spectrometry. From the determined astrocyte secretome, candidate proteins can be selected to test for synaptogenic potential.

I have tested two constructs expressing TurboID linked to ER retention sequences – KDEL and Sec61b. In commonly used cell lines, I validated the constructs by immunofluorescence and Western Blot analysis. In transfected cells, I observed the colocalisation of both constructs with the ER-resident protein calnexin. Additionally, I confirmed the presence of biotinylated proteins inside transfected cells and in their conditioned media. Moreover, in an astrocyte-like cell line, by increasing biotin incubation and chase times, I maximised the amount of biotinylated proteins that could be collected from the conditioned medium. Lastly, I used lentiviral vectors expressing the same constructs (TurboID-KDEL and Sec61b-TurboID) to transduce mouse primary astrocytes. Preliminary results show that TurboID is active in these transduced cells.

This work paves the way for this system to be used to obtain the secretome of mouse astrocytes, allowing the host group to choose candidate proteins and study their involvement in inhibitory and excitatory synapse formation.

Keywords: astrocytes, secretome, proximity biotinylation, synapse formation, TurboID

Table of Contents

List of Abbreviations

ADNF	Activity-Dependent Neurotrophic Factor
AMPA	α-amino-3-hydroxy-5-methyl-4-isoxazolepropionic acid
ASD	Autism Spectrum Disorder
ATCC	American Type Culture Collection
BDNF	Brain-Derived Neurotrophic Factor
BSA	Bovine Serum Albumin
Ck	Chicken
Chrdl1	Chordin like-1
CMV	Cytomegalovirus
Cx3cr1	CX3C motif chemokine receptor 1 gene
DAPI	4′,6-diamidino-2-phenylindole
DMEM	Dulbecco's Modified Eagle's Medium
DMSO	Dimethyl Sulfoxide
DOC	Deoxycholic Acid
E/I	Excitatory/Inhibitory
ECL	Enhanced Chemiluminescence
EPSP	Excitatory Post-Synaptic Potential
ER	Endoplasmic Reticulum
FBS	Foetal Bovine Serum
GABA	γ-aminobutyric acid
GFAP	Glial Fibrillary Acidic Protein
HEK	Human Embryonic Kidney
HIV-1	Human Immunodeficiency Virus 1
IF	Immunofluorescence
IgK	Light chain Kappa
IPSP	Inhibitory Post-Synaptic Potential

LC-MS/MS	Liquid Chromatography-tandem Mass Spectrometry
LB	Luria Broth
LTR	Long Terminal Repeat
LUTs	Look Up Tables
LV	Lentiviral Vector
Mbp	Myelin basic protein gene
m/v	mass/volume
mGluR	Metabotropic Glutamate Receptor
MP	Membrane Protein
MS	Mass Spectrometry
NMDA	N-methyl-D-aspartate
NRCAM	Neuronal Cell Adhesion Molecule
P	Post-Natal Day
PCR	Polymerase Chain Reaction
Pecam1	Platelet endothelial cell adhesion molecule gene
PEI	Polyethylenimide
PenStrep	Penicillin/Streptomycin
PES	Polyethersulfone
PFA	Paraformaldehyde
PL	Proximity Labelling
PMSF	Phenylmethanesulfonyl Fluoride
qPCR	Quantitative Polymerase Chain Reaction
SDS	Sodium Dodecyl-Sulfate
SDS-PAGE	Sodium Dodecyl-Sulfate Polyacrylamide Gel Electrophoresis
SP	Secreted Protein
SPARC	Secreted Protein Acidic and Rich in Cysteine
Syt1	Synaptotagmin 1

TBS-T	Tris-Buffered Saline with 0.1% Tween-20
TCA	Trichloroacetic Acid
LB	Luria Broth
LTR	Long Terminal Repeat
LUTs	Look Up Tables
TGF-β	Transforming Growth Factor beta
TNF-α	Tumour Necrosis Factor-alpha
Tsp1	Thrombospondin-1 gene
TSP	Thrombospondin
TUs	Transducing Units
v/v	volume/volume
WB	Western Blot
WT	Wild-Type

List of Figures

List of Tables

1. Introduction

1.1. Transmitting information across the Nervous System

The vertebrate Nervous System is a complex system specialised in processing and transmitting information both within the body and between the body and the surrounding environment. The Central Nervous System (CNS) comprises the brain and the spinal cord and can process and integrate information, inducing a response.[1] The correct development and functioning of the CNS involve highly dynamic and tuned cross-talk between different cell types: neurons, which transmit information, and glial cells. Glial cells include astrocytes, which have multiple functions in keeping the CNS balanced, including proper synapse assembly and maturation; microglia, the brain's immune cells; oligodendrocytes, which myelinate neurons; ependyma; and neuronal vasculature, essential in providing oxygen and nutrients to the brain.[2]

Neurons are specialised in receiving, processing, carrying, and transmitting information, forming complex neuronal networks. Neurons are heterogeneous cells with a polarised morphology. Although neuron morphology is very variable throughout the CNS, these cells comprise one end capable of receiving information from other neurons, an axon with variable lengths capable of conducting electric current, and terminals where information is transmitted to the following neuron. A signal is transmitted through a neuron through electric currents. Upon a stimulus, neurons are depolarised by Na^+ influx through voltage-gated channels, triggering an action potential that spreads throughout the axon. At the terminal, depolarisation by Ca^{2+} influx results in the release of neurotransmitters to the following neuron at a special contact point called a synapse.[1]

1.1.1. Synapses

Synapses are responsible for fast point-to-point information transfer between neurons. These structures are asymmetric intercellular junctions generally formed by a pre-synaptic neuron, responsible for Ca^{2+}-triggered neurotransmitter release via exocytosis, and a post-synaptic neuron, which has receptors for these neurotransmitters and is responsible for receiving information.

There are many different types of synapses that vary in their morphology, neurotransmitter types, release probability, receptors, and plasticity. The two major types of synapses are excitatory and inhibitory. Excitatory synapses generate excitatory post-synaptic potentials (EPSPs) with the entry of Na^+ through post-synaptic membrane channels. In contrast, inhibitory synapses generate inhibitory ones (IPSPs) that involve an influx of Cl^- to the post-synaptic neuron. It is the sum of these potentials that makes a neuron more or less

prone to excitation, with an action potential being triggered when the membrane potential exceeds a certain threshold.[3]

Regarding synapse morphology, pre-synaptic specialisations are generally formed by axon terminals, while post-synaptic specialisations are usually formed, for excitatory synapses, on dendritic spines and, for inhibitory synapses, in neuronal shafts and neuronal soma.[4,5]

There are numerous neurotransmitters that signal the post-synapse through membrane receptors. These receptors can be ionotropic, which induce a fastest response through ion permeability changes, or metabotropic, which trigger a slower response through a cascade of secondary messengers. The most common excitatory neurotransmitter is glutamate, and inhibitory are γ-aminobutyric acid (GABA) and glycine. Glutamate signals the post-synaptic site through ionotropic α-amino-3-hydroxy-5-methyl-4-isoxazolepropionic acid (AMPA), N-methyl-D-aspartate (NMDA) and kainite receptors, and metabotropic glutamate receptors (mGluR). GABA acts through ionotropic $GABA_A$ and metabotropic $GABA_B$ receptors. Other CNS neurotransmitters include monoamines, purines and acetylcholine.[3]

1.1.2. Synapse formation

Synapses form during early post-natal development in a dynamic process that starts with the alignment of pre- and post-synaptic neurons – structural synapse formation – followed by the assembly of both the pre-synaptic machinery necessary for synaptic vesicle exocytosis and neurotransmitter release, as well as the recruitment of neurotransmitter receptors to the post-synaptic membrane. This initial period of synapse formation is followed by a maturation phase, in which the synaptic response is modified.[6,7] A well-studied example on excitatory synapses are AMPA receptors. These receptors are recruited during structural synapse formation, initially containing calcium-permeable GluA1 subunits, that are replaced with GluA2 calcium-impermeable subunits as synapses become stable and mature.[6,8] Another example are NMDA receptors, for which downregulation of the NR3A subunit of this receptor is essential for synapse maturation.[9]

1.1.3. Excitatory/Inhibitory balance

During development and into adulthood, the balance between excitatory and inhibitory synapses is essential for the proper functioning of the Nervous System.

During neurodevelopment, changes in synapse formation, maturation, or elimination might lead to excitatory/inhibitory (E/I) imbalances and may result in various disorders.[5] Several neurodevelopmental disorders have been linked to E/I imbalances, including autism spectrum disorder (ASD), that could be associated with an increase in the excitation/inhibition

ratio on crucial neural systems.[10,11] Other disorders, such as epilepsy[12], Rett's syndrome[13], Down's Syndrome[14], schizophrenia[15], and attention deficit hyperactivity disorder (ADHD)[16] have also been associated with this type of imbalances.

1.2. Astrocytes

Astrocytes are the most abundant glial cell type in the mammalian brain. With a star-like morphology, these cells emit thousands of long and highly ramified processes and tile the whole brain parenchyma by occupying closely packed discrete territories. For a long time, the exact function of this type of glial cell was unknown. Firstly, considered to work as a type of "glue" for neuronal cells, then seen as mere support cells for the correct functioning of neurons, astrocytes are now known to communicate with a range of different cell types in the Nervous System, being essential for its correct development and functioning.[17–20]

Astrocytes are a heterogeneous cell population. There are two main types of astrocytes: protoplasmic, found in grey matter, with processes ensheathing synapses and blood vessels; and fibrous, which contact blood vessels and nodes of Ranvier in white matter. In addition to these two big groups, there are region-specific protoplasmic-like astrocytes, such as Müller glia in the retina or Bergman glia in the cerebellum.[18] Additionally, there are visible differences in GFAP and membrane receptor expression levels in different astrocytes. In addition to these clearly visible differences, astrocytes present differences regarding their molecular profile, developmental origin, physiology, and function, suggesting astrocyte heterogeneity both within and outside the same brain region.[17]

Astrocytes are crucial in regulating synapse formation and function, keeping metabolic support, ion and water homeostatic function of the CNS, and keeping the blood-brain barrier. These cells also contact nodes of Ranvier, and other glial cells.[2] Moreover, astrocytic processes present various neurotransmitter receptors that are used to regulate neuronal communication. For example, by expressing glutamate transporters, astrocytes can regulate the levels of glutamate at synapses, avoiding neuron hyperexcitability and neurotransmitter "spillover" to nearby synapses. Moreover, glutamate signalling through metabotropic glutamate receptors (mGluR5s) present in astrocytes can trigger Ca^{2+} transients, leading to the release of chemical mediators known as "gliotransmitters" that can modulate the actions of neurons, other glial cells or vascular cells. Transient Ca^{2+} increases in astrocytes can also occur independently from synaptic activity, especially at specific times during development.[19,21–23] Another function of astrocytes involves their ability to become reactive when there is some type of insult to the CNS, in a process called astrogliosis. Reactive astrocytes show changes in morphology, gene expression and function, resulting either in neuroprotective (A2) or neurotoxic (A1) reactive astrocyte types.[24,25]

1.3. The role of astrocytes on synapse formation

Astrocytes are closely associated with synapses, forming what we call a “tripartite synapse”. Due to its highly arborised structure, a single astrocyte can contact over 100 000 synapses in mice and up to 2 000 000 in humans.[23] This results in a high number of synapses being tripartite: with differences between brain regions, around 90% of synapses in the cortex and 86% in the hippocampus are tripartite.[17]

This close interaction between astrocytes and synapses starts early in CNS development. Astrocytes are generated by the same progenitors as neurons and oligodendrocytes: radial glia. In mice, right before birth, there is a switch from neurogenesis to astrogenesis that peaks right after birth and is finished at the end of the first postnatal week. This period overlaps with the time period in which synapses start being assembled, with both astrocytes and synapses showing mature morphology around three weeks after birth.[17,20] This led to the hypothesis that astrocytes could be important for synapse assembly. Since the early 2000s, several studies have shown the importance of astrocytes for synapse formation in various brain regions and different types of synapses.[26,27]

Many different astrocytic factors have been identified as necessary for synapse assembly, most of them being either secreted or membrane proteins. Different astrocytic factors act at different phases of synapse assembly and either at the pre- or post-synaptic sites. At the pre-synaptic site synaptic transmission can be modified by vesicle release probability or number of vesicles released in response to an action potential. Post-synaptic response varies depending on receptor number, stability, subunits and phosphorylation status.[28]

1.3.1. Excitatory synapses

A number of astrocytic proteins have been identified to play critical roles at all stages of the excitatory synapses' life cycle (*Table 1*). For example, the astrocyte-secreted guidance protein **semaphorin a3** plays a key role in axon orientation and the establishment of wiring patterns in motor fibres during development.[29] Additionally, several astrocytic membrane-associated proteins, like **γ-protocadherins** and **neuroligin-2,** bind their specific partners in the neuronal membrane, stabilising the structure of a synapse.[30–32] Finally, various astrocyte-secreted proteins have been proven essential for the formation of structural synapses,[29,33] as well for the initiation[34] and maintenance of functionally mature synapses. These proteins can impact both pre-[35–38] and post-synaptic function.[38–44] For example, **TSPs -1 and -2** are well-known for regulating synaptic formation. During early postnatal development, TSPs are crucial for the formation of immature post-synaptically silent synapses.[33] **Glypicans -4 and -6** increase post-synaptic surface levels and clustering of the GluA1-containing immature AMPA glutamate receptor[40], and **chordin-like 1**, at later stages of development, induces the

formation of GluA2-containing mature synapses.[43] Moreover, other astrocyte proteins, like **SPARC**, actually antagonise synapse formation.[34]

The formation and maintenance of excitatory synapses are, therefore, complex and very dynamic processes that largely depend on astrocytic proteins.

1.3.2. Inhibitory synapses

It is established that inhibitory synapses also depend on astrocytic proteins to properly form and function.[45] However, likely because of the low abundance of inhibitory synapses in various brain areas in comparison to excitatory ones, much less is known about the mechanisms by which inhibitory synapses are formed (*Table 1*).

Two astrocyte membrane proteins, **NRCAM** and **γ-protocadherins,** appear necessary for the formation of inhibitory synapses.[30,46] **BDNF** has also been reported to play a role in the pre-synaptic function of inhibitory synapses,[47] while the **neurocan** C-terminal fragment was recently proposed as an astrocyte secreted factor specifically promoting inhibitory synapse formation and function.[48] The role of **TGF-β** is contentious, with conflicting reports as to whether it promotes or inhibits inhibitory synapse formation.[49,50]

These studies indicate that the proteins involved in the formation of inhibitory synapses substantially differ from the ones responsible for excitatory synapse formation. Besides, based on the complexity of synapse formation and maturation and on the importance that astrocyte-neuron communication has on these processes, it is expected that a lot more astrocytic factors involved in the formation of synapses, especially inhibitory ones, are yet to be identified. Identifying these proteins is essential to our understanding of the mechanisms by which excitatory and inhibitory synapses are differently formed.

1.3.1. Association between astrocyte factors crucial for synapse formation and neurodevelopmental disorders

Moreover, many astrocytic factors crucial for synapse formation have been associated with neurodevelopmental disorders: Gpc6 mutations are connected to attention deficit hyperactivity disorder (ADHD)[51] and neuroticism[52], while deficits in TSP-1 expression have been associated with Down's Syndrome.[53] Additionally, in Rett's syndrome, loss of methyl-CpG–binding protein 2 (MeCP2) in astrocytes leads to an inability to support dendrite formation,[54] and fragile X astrocytes lead to impaired synapse formation in cultured neurons.[55]

Therefore, identifying more astrocytic factors involved in synapse formation may also help us understand the mechanisms behind several neurodevelopmental disorders.

***Table 1* – Known astrocyte factors modulating synapse formation and function.**

Factor	Class	Type(s) of synapse(s)	Function	Brain area	References
Ephrin-A3	MP	Excitatory	Dendritic spine morphology	Mouse hippocampus (*in vivo*)	31
			Glutamate transporters' expression		
Cholesterol	Lipid	Excitatory	Pre-synaptic differentiation	Rat retinal ganglion cells (*in vitro*)	35,36
Semaphorin a3	SP	Excitatory	Axon orientation	Mouse spinal cord (*in vivo*)	29
TSPs 1 and 2	SP	Excitatory	Induce structural synapse formation	Rat retinal ganglion cells (*in vitro*)	33
			Pre-synaptic muting	Rat hippocampal neurons (*in vitro*)	37
			AMPA and glycine receptor regulation	Rat spinal cord neurons (*in vitro*)	39
Hevin	SP	Excitatory	Structural synapse formation	Mouse superior colliculus (*in vivo*)	34
SPARC	SP	Excitatory	Hevin antagonist		
ADNF	SP	Excitatory	Pre-synaptic function	Rat hippocampal neurons (*in vitro*)	38

Glypicans -4 and -6	SP	Excitatory	Regulates post-synaptic AMPAR levels and subunits	Rat retinal ganglion cells (*in vitro*)	40
TNF-α	SP	Excitatory	Regulates post-synaptic AMPAR levels	Rat hippocampal neurons (*in vitro*)	41
Chordin-like 1	SP	Excitatory	Synaptic maturation: increases GluA2-containing AMPARs	Mouse visual cortex (*in vivo*)	43
Pentraxin-3	SP	Excitatory	Synaptic maturation: Post-synaptic AMPAR levels	Mouse hippocampal neurons (*in vitro*)	44
Neuroligin-2	MP	Excitatory (and inhibitory)	Synapse formation and function	Mouse visual cortex (*in vivo*)	32
γ-protocadherins	MP	Excitatory and inhibitory	Structural synapse formation	Mouse spinal cord (*in vivo*)	30
TGF-β	SP	Excitatory and inhibitory	Synapse formation through D-serine signalling	*Drosophila* neuromuscular junction (*in vivo*)	50
				Mouse cortical neurons (*in vitro*)	56,57

BDNF	SP	Excitatory and Inhibitory	Pre-synaptic function	Rat hippocampal neurons (*in vitro*)	47
NRCAM	MP	Inhibitory	Synapse formation	Mouse visual cortex (*in vivo*)	46
Neurocan	SP	Inhibitory	Synapse formation and function	Rat cortical neurons (*in vitro*)	48

SP – secreted protein; MP – membrane protein; TSPs – thrombospondins; SPARC – secreted protein acidic and rich in cysteine; ADNF – activity-dependent neurotrophic factor; TNF-α – tumour necrosis factor-alpha; TGF-β – transforming growth factor beta; NRCAM – neuronal cell adhesion molecule; BDNF – brain-derived neurotrophic factor.

1.4. Surveying cell-specific secretome

Surveying the secretome of a specific cell type, i.e. identifying the biggest and most accurate possible pool of proteins that are secreted from those cells, can be complex and laborious.

Most secretome studies have been conducted *in vitro*. In these studies, conditioned medium from cultured cells is collected and concentrated. After this, using different chromatography approaches, proteins can be separated into different fractions to ensure the identification of the maximum possible amount of secreted proteins. Proteins on these fractions are then, after digestion with trypsin, identified by liquid chromatography-tandem mass spectrometry (LC-MS/MS). To do this without the interference of serum proteins present in the culture medium, cells must be kept in serum-free medium while secreting proteins for collection. Depending on the cell type, this cannot be done for long periods without damaging cell health and possibly altering their secretome. Moreover, cell lysis, which could be increased due to higher cell death in serum-free conditions, can contaminate the sample with intracellular proteins that can hide low-abundant secreted proteins in the analysis.[58,59]

In vivo, secretome studies are much more complex, involving comparisons between the proteomes of specific body fluids and cell-specific proteome databases. Moreover, in the brain, this type of analysis usually involves complex microdialysis techniques.[59,60]

1.5. Proximity labelling

Proximity labelling (PL) enzymes can be genetically delivered to cells. Inside or on the surface of live cells, the enzyme catalyses the addition of a label molecule to proteins in its close vicinity. This technology can be used either in cultured cells or *in vivo*.

PL is, therefore, a very useful molecular tool for various applications, such as studying protein-protein interactions or profiling local DNA or RNA pools. Moreover, PL has been largely employed to study “molecular spaciomics” in live cells. This is done by directing the enzyme to specific locations inside or on the surface of cells by fusing it to specific signal peptides or proteins that can direct it to the desired location. Labelled proteins can then be easily isolated and identified by mass spectrometry (MS). This allows the characterisation of local proteomes in different cell locations.[61,62]

1.5.1. Biotinylating enzymes

One of the most commonly used types of proximity labelling enzymes are biotinylating enzymes. As they use biotin as the labelling molecule, labelled proteins can be easily purified using biotin-streptavidin affinity. As biotin and streptavidin have a very strong interaction, biotinylated proteins can be enriched using streptavidin beads: biotinylated proteins bind to

the beads while non-biotinylated ones are removed, biotinylated proteins are then eluted, and this sample can be analysed by mass spectrometry to identify the proteins that were biotinylated.[61,63]

Biotinylating enzymes used in these type of studies have been engineered from wild-type enzymes isolated from bacteria or plants. Several different biotinylating enzymes have been engineered. Each with different advantages and limitations, the right enzyme should be chosen according to the specific goal of a study.[62]

Biotinylating enzymes can be divided into two large groups: biotin ligases and peroxidases.

1.5.1.1. Peroxidases

Peroxidases include Horseradish Peroxidase (HRP) and Ascorbate Peroxidase (APEX) and enhanced or further engineered versions of these enzymes. When activated by oxygen peroxide (H_2O_2), peroxidases can convert biotin-phenol into a highly reactive but very short-lived (< 1 ms) radical capable of covalently binding electron-rich tyrosine residues from nearby proteins. These enzymes have very short (1 to 10 minutes) optimal labelling times and the advantage that labelling can be stopped by removing H_2O_2. A big limitation of these enzymes relies on the fact that their activity depends on H_2O_2, which can induce oxidative stress and is toxic to cells.[62,64]

1.5.1.2. Biotin ligases

Biotin ligases, like BioID or BioID2, need ATP to catalyse the conversion of biotin into reactive biotinoyl-5'-AMP that is then added to lysine residues on close-by proteins (~10 nm radius). This reactive intermediate has a longer half-life (minutes) when compared to biotin-phenoxyl radical, which can make the labelling radius larger. Moreover, a big limitation of BioID is that it has very long labelling times (15h-18h). However, this problem has been overcome in a recently engineered biotin ligase – TurboID – that has more affinity to biotin, labelling the same amount of protein in just 10 minutes. TurboID, besides having much faster labelling kinetics in comparison to BioID, is much more active in the ER than BioID and functions at broader temperatures. However, TurboID does have a higher affinity for biotin, and this may have unintended consequences, including the sequestration of endogenous biotin, which may lead to non-specific (background) labelling of proteins or cell toxicity.[59,65,66]

1.5.2. Applying proximity labelling to survey cell-specific secretome

As the majority (if not all) proteins secreted by mammalian cells transit through the endoplasmic reticulum (ER), proximity labelling enzymes can be directed and retained in the lumen of this organelle. Labelled proteins will then be secreted into the medium, collected, easily purified using streptavidin beads, and identified using LC-MS/MS.

These was done by Liu and colleagues in 2020. They use the biotin ligase BioID2 linked to the murine kappa light chain leader sequence (IgK leader) – to drive it to the secretory pathway –, and the KDEL sequence – to retain it inside the ER. In this study they determined, *in vitro*, the secretome of endothelial cells, and *in vivo* the secretome of both mice endothelial and muscular cells.[60]

Additionally, in 2021, Kim and colleagues use TurboID linked to Sec61b to obtain the liver mouse secretome *in vivo*. Sec61b is an ER membrane protein with its C-terminal facing the lumen of the ER. Linking TurboID to the C-terminal of this protein can therefore direct it to the ER lumen.[67]

1.7. Objectives of this work

As mentioned before, identifying which astrocytic proteins modulate excitatory and inhibitory synapses is an essential step into understanding how they are formed and unravelling the mechanisms behind several neurodevelopmental disorders.

With this in mind, I aimed to develop a protein biotinylation system that could be used to unravel the astrocyte-specific secretome, so candidate proteins can subsequently be tested for synaptogenic potential.

To do this, I tested two different constructs: IgK-TurboID-KDEL and Sec61b-TurboID (*Figure 1*).

In summary, I aimed to:

1) In cells expressing IgK-TurboID-KDEL or Sec61b-TurboID confirm that:
   - TurboID-KDEL and Sec61b-TurboID colocalise with the ER;
   - TurboID is active;
   - biotinylated proteins are secreted into the culture medium and can be collected.
2) Check if increasing incubation times with biotin or chase times could increase the amount of biotinylated proteins collected from conditioned media.
3) Assess if the system could be applied to primary astrocytes.

2. Materials and Methods

2.1. Cell lines: COS-7, HEK-293T and C8-D1A cells

COS-7, human embryonic kidney (HEK) 293T and C8-D1A cells (American Type Culture Collection; ATCC) grown and maintained in Dulbecco's Modified Eagle's Medium (DMEM) with GlutaMAX, high glucose, sodium pyruvate and phenol red (Gibco, ThermoFisher Scientific) supplemented with 10% (v/v) heat-inactivated foetal bovine serum (HI-FBS; Gibco, ThermoFisher Scientific) and 1% (v/v) penicillin/streptomycin (PenStrep, Gibco, ThermoFisher Scientific), at 37ºC and 5% CO_2. Every 3 to 5 days, cells were dissociated using 0.25% Trypsin-EDTA (Gibco, ThermoFisher Scientific) and pelleted by centrifuging for 5 minutes at 3000 x g to remove the trypsin. Pelleted cells were then resuspended in fresh medium, and 1:10 of the cells were re-plated in a new medium.

2.2. Primary astrocytes

The protocol for mouse primary astrocyte cultures was established based on previously published protocols.[68,69]

Primary mouse astrocytic cultures were prepared from cortices of post-natal day (P)1 C57BL/6 wild-type (WT) mice. During the dissection of brains and right after dissection, cortices were kept in HBSS (Hanks' Balanced Salt Solution, $+Mg^{2+}$ $+Ca^{2+}$, no phenol red). Tissue was then washed with HBSS (no Mg^{2+}, no Ca^{2+}, with phenol red), cut, and digested. Cortices were cut into pieces and digested by adding 3 mL of 0.0025% Trypsin-EDTA and 30 µL of 0.005 mg/mL DNase to the same medium. Tissue was incubated in this media for 15 to 20 minutes at 37ºC, shaking every 5 minutes, and then thoroughly homogenised before stopping the digestion with culture medium (DMEM + 10% FBS + 1% PenStrep). Large cell clusters were removed using a 40 µm nylon cell strainer. Cells were then centrifuged at 304 x g for 5 minutes at room temperature (RT), pelleted cells resuspended in fresh culture medium, and around 1 x 10^7 cells plated in pre-poly-D-lysine(PDL)-coated T75 flasks and kept in culture at 37ºC and 5% CO_2. One and 3 days after plating, the culture medium was changed to a fresh one. When cells were 80-90% confluent, they underwent mechanical orbital shaking (Infors AG CH-4103 Bottmingen, 150 rpm, 37ºC) for 3 hours to remove non-astrocytic cells. This shaking protocol was repeated after 7 and 14 days. After the third shake, astrocytes were trypsinised (0.25% Trypsin-EDTA) and pelleted by centrifuging for 5 minutes at 3000 x g to remove the trypsin. Pelleted cells were then resuspended in fresh medium and re-plated in a new PDL-coated T75 flask. This was repeated every time cells reached 80-90% confluency.

Astrocyte purity was accessed by immunofluorescence (IF) by staining for GFAP, an astrocyte-specific marker, and nuclei (4′,6-diamidino-2-phenylindole; DAPI) – the percentage

of astrocytes was calculated by dividing the number of positive GFAP cells for the total cell number (stained with DAPI). qPCR (quantitative polymerase chain reaction) was used to assess changes in the expression of specific markers in the primary cultures compared to a whole cortex tissue sample. qPCR was performed for cell-type specific mRNAs – Glial fibrillary acidic protein (*GFAP*) for astrocytes;[70] Myelin basic protein (*Mbp*) for oligodendrocytes;[71] Synaptotagmin 1 (*Syt1*) for neurons;[72] CX3C motif chemokine receptor 1 (*Cx3cr1*) for microglia;[71] Platelet endothelial cell adhesion molecule (*Pecam1*) for endothelial cells;[73] and synaptogenic astrocyte secreted proteins – glypican-4 (*Gpc4*),[40] thrombospondin-1 (*Tsp1*)[33] and chordin like-1 (*Chrdl1*)).[43] Purity assays were performed by João Guimarães, a PhD student from the host Laboratory.

2.3. Cell line transfection

COS-7 and HEK-293T cells were transfected with either pMX-IgK-TurboID-V5-KDEL (ATCC) or pcDNA5-Sec61b-V5-TurboID (addgene #166971) using polyethylenimide (PEI; Polysciences inc.) as transfection reagent at a 1:3.5 DNA to PEI mass/mass ratio. To prepare the transfection medium, a 200 µL solution was prepared by carefully mixing DNA with a PEI solution, both in 100 µL of 150 mM NaCl. For cells in 24-well plates, 1 µg of DNA per well was used to transfect COS-7 cells, while only 0.5 µg was needed for HEK-293T cells. For HEK-293T cells in 6-well plates, 3 µg of DNA were used for each well. The transfection solution was added to cells in fresh DMEM supplemented with only 1% FBS and left for 5 hours, after which the media was changed to a fresh culture medium (see *2.1. Cell lines*). Cells were collected or further treated only 24 hours after transfection to allow protein expression.

Due to low transfection rates using PEI, C8-D1A cells were transfected using Lipofectamine 3000 Reagent (Invitrogen, ThermoFisher). Transfection was carried out according to the manufacturer's protocol for a 6-well plate. To prepare a 250 µL transfection solution for each well, two solutions were mixed: 2.5 µg of DNA and 5 µL of P3000 Reagent in 125 µL of Opti-MEM I (Thermo Fisher Scientific); and 7.5 µL of Lipofectamine 3000 Reagent in 125 µL of Opti-MEM I. The mix was incubated for 15 minutes at RT and added to cells in fresh medium.

2.4. Immunofluorescence

Before cell seeding, sterilised coverslips were placed in 24-well plates and coated with PDL for cell adhesion. 35 000 to 50 000 COS-7 cells were seeded in each well and transfected 24 hours later, as described above. Twenty-four hours after transfection, cells were either fixed using 4% (m/v) paraformaldehyde (PFA) for 15 minutes right away, or treated with 100 µM biotin for one hour at 37°C before fixation. A 250 mM biotin solution was previously prepared in dimethyl sulfoxide (DMSO) using biotin lyophilised powder (Merck Life Science #B4501) and diluted in culture media before usage. For permeabilisation and blocking, cells were incubated with 3% bovine serum albumin (BSA) and 0.3% Triton X-100 in PBS for 1 hour at RT. Cells were then left overnight with primary antibody (*Table 2*) at 4°C. The next day, cells were incubated with a secondary antibody (*Table 2*) for 1 hour at RT. Cells were washed 3 times with PBS between every incubation. After nuclei staining using 1 µg/mL DAPI in PBS, coverslips were mounted on microscope slides using Fluoromount-G (0100-01, Southern Biotech).

Imaging was performed on the Zeiss Axio Imager Z1 upright epifluorescence microscope, using the Zeiss EC Plan-NEOFLUAR 40x/1.3 Oil DIC Microscope Objective and Axiocam MR ver3.0 (Carl Zeiss, Germany) camera. Depending on the secondary detection reagent used the following Zeiss filter sets were used: 49 (excitation: 365; emission: 445/50) for DAPI; 38HE (excitation: 470/40; emission: 525/50) for Alexa 488; 43HE (excitation: 550/2; emission: 605/70) for Cyanine Cy3 and streptavidin-Texas Red; and 50 (excitation: 640/30; emission: 690/50) for streptavidin-647.

Maximum projection of the z-stack images obtain were analysed using the Fiji software. For cells transfected with the same plasmid, exposure time and Look Up Tables (LUTs) were kept constant for biotinylation signal. Images were constructed on Adobe Illustrator.

***Table 2* – Detection reagents used for immunofluorescence.**

Primary antibodies				
Target	**Host species**	**Clonality**	**Reference**	**Dilution**
Calnexin	Rabbit	Monoclonal (C5C9)	Cell signalling #2679	1:100
V5 Tag	Mouse	Monoclonal (SV5-Pk1)	Invitrogen #R96025	1:500
HA-tag	Mouse	Monoclonal (16B12)	Biolegends #901501	1:500
GFAP	Guinea pig	Polyclonal	Synaptic Systems Antibodies #173004	1:300
Secondary antibodies				
Antibody	**Host species**	**Fluorophore**	**Reference**	**Dilution**
anti-Rabbit	Goat	Alexa 488	Jackson ImmunoResearch #111-545-144	1:200
anti-Mouse	Goat	Cyanine Cy3	Jackson ImmunoResearch #115-165-146	1:200
anti-Mouse	Goat	Alexa 488	Jackson ImmunoResearch #115-545-146	1:200
anti-Guinea Pig	Goat	Alexa 488	Jackson ImmunoResearch #106-545-003	1:200
Secondary detection reagents				
Streptavidin	-	TexasRed	Invitrogen #S872	1:200
Streptavidin	-	Alexa 647	Jackson ImmunoResearch #016-600-084	1:200

2.5. Electrophoresis and Western Blotting

Sample preparation:

For Western Blot (WB) analysis, 500 000 HEK 293T or C8-D1A cells were seeded in each 6-well plate well, transfected the next day as described above, and incubated with 100 µM biotin at 37ºC 24 hours later. Media were collected, and after two washes with PBS cells were scrapped from the wells using RIPA buffer (25 mM Tris pH 7.6, 150 mM NaCl, 1% IGEPAL, 1% Sodium deoxycholate, 0.1% sodium dodecyl-sulfate (SDS) in water) supplemented with protease inhibitors – 1 µM pepstatin, 1 mM Phenylmethanesulfonyl fluoride (PMSF) and phosphatase inhibitor (1x PhosSTOP). Samples were then sonicated for 30 seconds (3x 10 seconds) with high pulse and centrifuge at 18 000 x g for 20 minutes at 4ºC, and supernatants were collected. Medium samples were centrifuged at 400 x g for 5 minutes and filtered using a 0.2 µm polyethersulfone (PES) syringe filter (VWR #28145-501) before concentrating around 20 times (in volume) using Vivaspin 3 kDa columns (GE Healthcare). Samples were stored at -80ºC.

Protein determination:

Protein concentration in samples was determined using the modified Lowry-Peterson method.[74] In this method, after the addition of 100 µL of 0.15% (m/v) deoxycholic acid (DOC) to protein samples previously diluted in 1 mL of water, proteins were precipitated by adding 100 µL of 72% (m/v) trichloroacetic acid (TCA), on ice, leaving it for 5 minutes before centrifuging at 16 000 xg for 10 minutes at 4ºC. Pelleted protein was resuspended in 1 mL of Reagent A (1.5% (m/v) Na_2CO_3, 0.3% (m/v) NaOH, 0.12% (m/v) Na_2-Tartate x2 H_2O, 0.75% (m/v) SDS, and 0.03% (m/v) $CuSO_4$ x5 H2O), and kept at room temperature for 30 minutes in the dark, after which 75 uL Reagent B (50% (v/v) Folin-Ciocalteus-Phenol) was added. After a 45-minute incubation at RT in the dark, absorbance was read on a spectrophotometer (UltraSpec 100 Pro) at 750 nm. A standard curve was done using serial dilutions of BSA (Pierce™ Bovine Serum Albumin Standard Ampules, Thermo Fisher Scientific), and the protein concentration of each sample was calculated using the equation of the curve.

Gel electrophoresis:

20 ug of protein were mixed with Laemmli SDS sample buffer (62.5 mM Tris pH 7.6, 1.5% (m/v) SDS, 8.3% (v/v) glycerol, 1.5% 2-mercaptoethanol (v/v), 0.0125% bromophenol blue (m/v) in water), and denaturated at 95 ºC for 5 minutes. Sodium dodecyl-sulfate polyacrylamide gel electrophoresis (SDS-PAGE) was performed using a Mini Protean Tetra System (Bio-Rad). PageRuler Prestained Protein Ladder (Thermo Fisher Scientific) was used for size standards. Samples were loaded in an SDS-PAGE gel (4% stacking; 12% resolving),

and electrophoresis was performed at the constant voltage of 80 V for protein stacking, followed by 125 V for protein separation. Tris-glycine (25 mM Tris, 192 mM glycine in water, pH 8.8) with 1% SDS was used as Running Buffer.

Protein transfer:

Proteins were then transferred from the gel to a 0.45 µm nitrocellulose membrane (Amersham Protran) by Wet Transfer using a Mini-Protean Tetra Cell with a Mini Trans-Blot Module System (Bio-Rad). Tris-glycine with 20% methanol was used as Transfer Buffer, and transferring was carried out for 90 minutes at constant voltage (100 V). Membrane was stained with Ponceau S 0.1% (in 5% Acetic Acid Glacial in water) to confirm proper protein transfer.

Western Blotting:

After washing with Tris-Buffered Saline (25 mM Tris-HCl, 2.7 mM KCl, 137 mM NaCl in water, pH 7.4) with 0.1% Tween-20 reagent (TBS-T), the membrane was blocked for one hour using 5% milk powder in TBS-T. The membrane was then incubated with primary antibody (*Table 3*) overnight at 4^{o}C, under gentle shaking. After three 5-minute and three 10-minute washes with TBS-T, the membrane was incubated with a secondary antibody (*Table 3*) for one hour at RT, under gentle shaking. Secondary antibody solutions were prepared in 5% Milk, with the exception of streptavidin-HRP and streptavidin-647, which were prepared in 1% BSA in TBS-T. After three 5-minute and three 10-minute washes, imaging for enhanced chemiluminescence (ECL) was done using the Bio-Rad Chemidoc MP imaging system after a 2-minute incubation with the Bio-Rad Clarity Western ECL Substrate. ECL images were processed using the ImageLab software. For fluorescent detection, the Odyssey CLx Infrared Imaging System and the ImageStudio Software were used. Images were exported as Tagged Image File Format (TIFF) files and further processed on the Fiji software. Signal quantification was performed using the ImageStudio Software, and images were constructed on Adobe Illustrator.

***Table 3* – Detection reagents used for Western Blot.**

Primary antibodies				
Target	**Host species**	**Clonality**	**Reference**	**Dilution**
β-actin	Rabbit	Monoclonal (13E5)	Cell Signalling #49705	1:2000
V5 Tag	Mouse	Monoclonal (SV5-Pk1)	Invitrogen #R96025	1:2000
Secondary antibodies				
Antibody	**Host species**	**Signal**	**Reference**	**Dilution**
Anti-Rabbit	Goat	800 IRDye	Rockland/TEBU BIO #611-132-122	1:10 000
Anti-Mouse	Goat	800 IRDye	LI-COR #926-32210	1:20 000
Secondary detection reagents				
Streptavidin	-	HRP	Jackson ImmunoResearch #016-030-084	1:1000
Streptavidin	-	Alexa 647	Jackson ImmunoResearch #016-600-084	1:1000

2.6. Plasmid constructs

The plasmids for lentiviral vector production – pFUGW-gfa2-IgK-TurboID-HA-KDEL and pFUGW-gfa2-Sec61b-V5-TurboID – were assembled using the FUGW-eGFP plasmid (kindly provided by Luís Ribeiro, CNC – Center of Neurosciences and Cell Biology of the University of Coimbra; addgene #14883) as backbone. Firstly, pFUGW-gfa2, a pFUGW backbone with the 2.2 kb human GFAP promoter (gfa2; (Lee et al., 2008)), was generated by digesting pFUGW-eGFP with the FastDigest restriction enzymes PacI and EcoRI (Thermo Fisher Scientific) at 37ºC for 30 minutes to remove the UbC promoter and eGFP sequences. After confirming the correct size by running the digest on an agarose gel, the digested DNA was purified using the QIAquick Gel Extraction Kit (Qiagen) according to the manufacturer's instructions and quantified at the Nanodrop 1000 at 260 nm. DNA was considered pure for 260/230 and 260/280 absorbance ratios above 1.8. The gfa2 promoter was amplified by polymerase chain reaction (PCR) using the pAAV-GFAP(2.2)mIL1RN-WPRE (Vector Biolabs) as a template, the In-fusion primers on *Table 4*, the Phusion High-Fidelity DNA polymerase (Thermo Fisher Scientific, #F530S), and the following cycling parameters: a 30-second initial denaturation at 98ºC; 35 cycles of: a 10-second denaturation at 98ºC, a 15-second annealing phase at 60ºC and a 30-second extension at 72ºC; a final extension step of 5 minutes at 72ºC. Correct insert amplification was confirmed by running it on an agarose gel. DNA was purified and quantified, as previously mentioned. The gfa2 promoter was inserted into the digested backbone using the In-fusion HF enzyme (Takara Bio), according to the manufacturer's instructions. The In-Fusion reaction was then transformed in One Shot™ Stbl3™ Chemically Competent E. coli (Invitrogen, Thermo Fisher) according to the manufacturer's instructions and grown on Luria Broth (LB)/ampicillin medium plates overnight at 30ºC. Colonies were inoculated and grown in liquid LB medium overnight at 200 rpm and 30ºC. Plasmid DNA was then extracted and purified using the GeneJET plasmid Miniprep Kit. Positive colonies were selected by restriction digestion (with PacI and EcoRI), and sequence was confirmed by Sanger sequencing using the primers in *Table 5*.

pFUGW-gfa2-IgK-TurboID-HA-KDEL and pFUGW-gfa2-Sec61b-V5-TurboID were generated using pFUGW-gfa2 as backbone. The plasmid was digested with EcoRI. Inserts were amplified by PCR with the primers in *Table 4*, and pMX-IgK-TurboID-V5-KDEL or pcDNA5-Sec61b-V5-TurboID as templates. In-fusion cloning, transformation, extraction and purification were performed as described above, and Sanger sequencing was done using the primers in *Table 5*.

Plasmids were generated by João Guimarães, a PhD student from the host Laboratory.

***Table 4* – Primers used for plasmid cloning.**

Plasmid construct	Orientation	Sequence (5' -> 3')
pFUGW-gfa2	Forward	GCAGAGATCCAGTTTGGTTAATTAATCC CACCTCCCTCTCTGTG
	Reverse	GCTTGATATCGAATTCTGCTCTGGCTCT GCTCGC
pFUGW-gfa2-IgK-TurboID-HA-KDEL	Forward	AGCAGAGCCAGAGCAGAATTCATGGAG ACAGACACACTCCTGC
	Reverse	GATAAGCTTGATATCGAATTCTCACAGCT CGTCCTTAGCATAATCTGGAACATCATAT GGATACTTTTCGGCAGACCGCAGAC
pFUGW-gfa2-Sec61b-V5-TurboID	Forward	AGCCAGAGCAGAATTCATGCCTGGTCCG ACCCCC
	Reverse	GCTTGATATCGAATTCTCACTTTTCGGCA GACCGC

***Table 5* – Primers used for plasmid sequencing.**

Plasmid construct	Orientation	Sequence (5' -> 3')
pFUGW-gfa2-IgK-TurboID-HA-KDEL	Forward	GGTTTATTACAGGGACAGCAG
	Reverse	CATTAAAGCAGCGTATCCACATAG
pFUGW-gfa2-Sec61b-V5-TurboID	Forward	GGTTTATTACAGGGACAGCAG
	Reverse	CATTAAAGCAGCGTATCCACATAG
	Forward	TGGTTATGAGTCTTCTGTTCATCG
pFUGW-gfa2	Forward	GGTTTATTACAGGGACAGCAG
	Reverse	CATTAAAGCAGCGTATCCACATAG
	Forward	CCAAGGACACAAATGGGTGAGG
	Forward	TATTCAGGAGGCTGAGGTGAG
	Forward	AAGCAGACCTGGCAGCATTG
	Reverse	CTGGAGACTTCAGGTCCATC

2.7. Production of lentiviral vectors

Lentiviral vectors were produced by transfecting HEK-293T cells with three plasmids: pVSV-G (addgene #138479), psPAX2 (addgene #12260**;** plasmids kindly provided by Luís Ribeiro, CNC), and a transfer plasmid with the DNA we want to deliver to the cells (pFUGW-gfa2-IgK-TurboID-HA-KDEL or pFUGW-gfa2-Sec61b-V5-TurboID). Protocol was adapted from addgene.

HEK-293T cells in T25 or T75 plates were transfected with 0.4 µg/mL of pVSV-G, 0.8 µg/mL of psPAX2, and 1 µg/mL of the transfer plasmid. Transfection was done using PEI as a transfection reagent, and a 1:3 DNA/PEI mass ratio. For the transfection two 200 µL intermediate solutions were prepared: one with the plasmids and the other with the PEI, both in Opti-MEM I. Solutions were mixed, and the mixture was incubated at RT for 20 minutes and then added to cells in DMEM with 10% FBS (but no antibiotics). Twenty-four hours later, the medium was changed to fresh DMEM with 10% FBS. Three days after transfection the medium was collected and centrifuged at 500 x g for 5 minutes to pellet cells that could be in suspension. The supernatants with the lentiviral vectors were filtered through a 0.45 µm PES syringe filter (ThermoFisher Scientific), aliquoted, snap-frozen in liquid N_2 and stored at -80ºC. When in use, lentiviral vectors were kept at 4ºC for a maximum of 24 hours.

2.8. Titering of lentiviral vectors

The number of transducing units per mL (TUs/mL) was determined by transducing C8-D1A cells with serial dilutions of lentiviral vectors and quantifying the number of lentiviral DNA copies per cell. To do this, qPCR of lentiviral vector-specific genes, Woodchuck Hepatitis Virus Posttranscriptional Regulatory Element (*WPRE*) and HIV-1 Rev response element (*RRE*), was performed. Albumin was used as a housekeeping gene.[75]

50 000 cells were plated into each well of a 24-well plate. 0, 1:10, 1:25 or 1:50 (v/v) lentiviral vectors in DMEM with 10% FBS and 8 ug/mL of polybrene were added to the cells. Three days later, cells were collected, and DNA was extracted using the NZY Tissue gDNA Isolation Kit (NZY Tech). DNA concentration was determined using the Nanodrop 1000, and 25 ng of DNA was used to perform qPCR for WPRE and/or RRE and albumin genes using the primers in *Table 2*. *Albumin* was used as a housekeeping gene so we could get the number of *WPRE*/*RRE* copies per cell. To quantify the number of copies in each sample, a standard curve was prepared from serial DNA dilutions (pFUGW for WPRE/RRE; DNA extracted from C8D1A cells for albumin). Since each cell has two albumin alleles, an average number of WPRE

copies per cell was determined by multiplying the WPRE/albumin ratio by 2. This number was then multiplied by the number of cells in a well and divided by the lentiviral volume added to said well, giving us the TUs/mL. The values used for subsequent experiments are the average of the TUs/mL obtained for each dilution.

Titering was performed by Simone Bessa, a Technician from the host Laboratory.

2.9. qPCR

qPCR was performed on a CFX96 Touch™ Real-Time PCR Detection System (Bio-Rad), using PowerUP SYBR™ Green Master Mix (Thermo Fisher Scientific), the primers on *Table 6*, and the following cycling parameters: 1 cycle at 95ºC for 3 minutes; 40 cycles at 95ºC for 10 minutes and 60ºC for 30 seconds; and 1 cycle at 95ºC for 15 seconds. Duplicates were performed for each condition.

***Table 6* – Primers used for qPCR.**

Gene	Forward primer (5' to 3')	Reverse primer (5' to 3')
Tbp	GCCAAGAGTGAAGAACAATCCA	AGAACTTAGCTGGGAAGCCC
Cyc1	TGCTCTTCCTGCCACAGC	GACCTCCACCTCCTCAGCC
Gfap	CTGCGTATAGACAGGAGGCAG	CTCCTCCTCCAGCGATTCAAC
Cx3cr1	CGTGAGACTGGGTGAGTGAC	GGACATGGTGAGGTCCTGAG
Mbp	CATCCTTGACTCCATCGGGC	CAGGGTACCTTGCCAGAGC
Syt1	GGGGAAGGGAAGGAAGATGC	ACGGTGGCAATGGGATTTTATG
Pecam1	AGCCAACAGCCATTACGGTTA	CTTCCGTTCTCTTGGTGAGGC
Gpc4	GTGCTTGGGAGAGAGGACCA	TATCATCCAGAGCAACGCCC
Thbs1	CAGAATGTGAGGTTTGTCTTTGG	TCAGTTCCAGGACCATGCTG
Chdrl1	TTTCAGAACCGGCAACCCAAT	TGGGAATGCACAGGTCAGTTT
WPRE	GTCCTTTCCTTGGCTGCTC	CCGAAGGGACGTAGCAGA
RRE	TTCTTGGGAGCAGCAGGAAG	GCCTCAATAGCCCTCAGCAA
Albumin	ACTATGGTGAACTGGCTGACTG	GGGTTGTCATCTTTGTGTTGCA

2.10. Transduction of primary astrocytes

Primary astrocytes were plated in 24-well plates on PDL-coated coverslips or directly in 6-well plates. Three days later, cells were transduced by adding the lentiviral vectors produced in *Methods 2.8.* diluted in complete DMEM (DMEM + 10% FBS + 1% PenStrep) directly to the cells to reach a multiplicity of infection (MOI) of 10 TUs per cell. The medium was changed the next day. To allow genome integration and protein expression, experiments were started seven days after transduction.

3. Results

3.1. System validation in cultured cell lines

The aim of my project was to develop a protein biotinylation system that could be used to unravel the astrocyte-specific secretome. For this, I tested two ER-retained TurboID designs: IgK-TurboID-KDEL and Sec61b-TurboID (*Figure 1*). The objective of this system is that TurboID-KDEL and Sec61b-TurboID are successfully retained in the ER so they can specifically biotinylate proteins in the ER lumen. These proteins will then be secreted, and we should be able to collect them from the cell medium.

Using common cell lines, the first task of my project was to validate two plasmids expressing the cassettes shown in *Image 1* with a V5 epitope tag: pMX-IgK-TurboID-V5-KDEL and pcDNA5-Sec61b-V5-TurboID (plasmid maps on *Supplementary Information*).

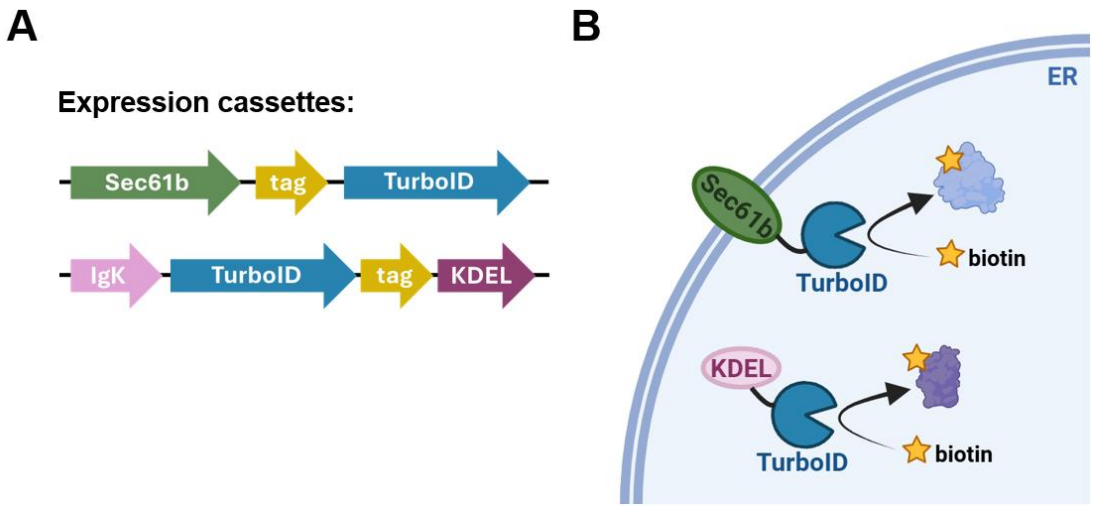

***Figure 1* – Biotinylation of ER proteins using Sec61b-TurboID and TurboID-KDEL.** (A) Basic design for expression cassettes expressing ER-resident TurboIDs – Sec61b-tag-TurboID and IgK-TurboID-tag-KDEL. (B) Schematic representation of biotinylation of ER proteins by Sec61b-TurboID and TurboID-KDEL. Figure constructed using BioRender.

3.1.1. TurboID-KDEL and Sec61b-TurboID colocalize with an ER resident protein

Firstly, I used immunofluorescence to confirm that TurboID-KDEL and Sec61b-TurboID are retained in the ER.

For this set of experiments I used the COS-7 cell line, a monkey kidney fibroblast-like cell line. These cells are very flat, which is advantageous to clearly see the ER. Cells were transfected with either pMX-IgK-TurboID-V5-KDEL or pcDNA5-Sec61b-V5-TurboID and 24 hours later fixed. Cells were then stained for the V5 epitope tag linked to TurboID and the ER resident protein calnexin to check for colocalization.

As shown in *Figure 2*, in both cells transfected with pMX-IgK-TurboID-V5-KDEL and pcDNA5-Sec61b-V5-TurboID, the V5 tag colocalises with calnexin, confirming that both TurboID-KDEL and Sec61b-TurboID are retained in the ER.

3.1.2. TurboID-KDEL and Sec61b-TurboID biotinylate proteins in the secretory pathway

After confirming that TurboID was successfully being retained in the ER, I used the same cell line to assess that the enzyme was active. To do this, one day after transfection, cells were treated with 100 µM biotin for one hour at 37ºC. Cells were then fixed and stained for the V5 epitope tag and with a streptavidin conjugate to mark biotinylated proteins.

For cells transfected with both pMX-IgK-TurboID-V5-KDEL and pcDNA5-Sec61b-V5-TurboID, biotinylation was observed only on transfected cells, and specifically upon biotin addition (*Figure 3*). This demonstrates that when cells are exposed to excess exogenous biotin, TurboID biotinylates proteins in its vicinity.

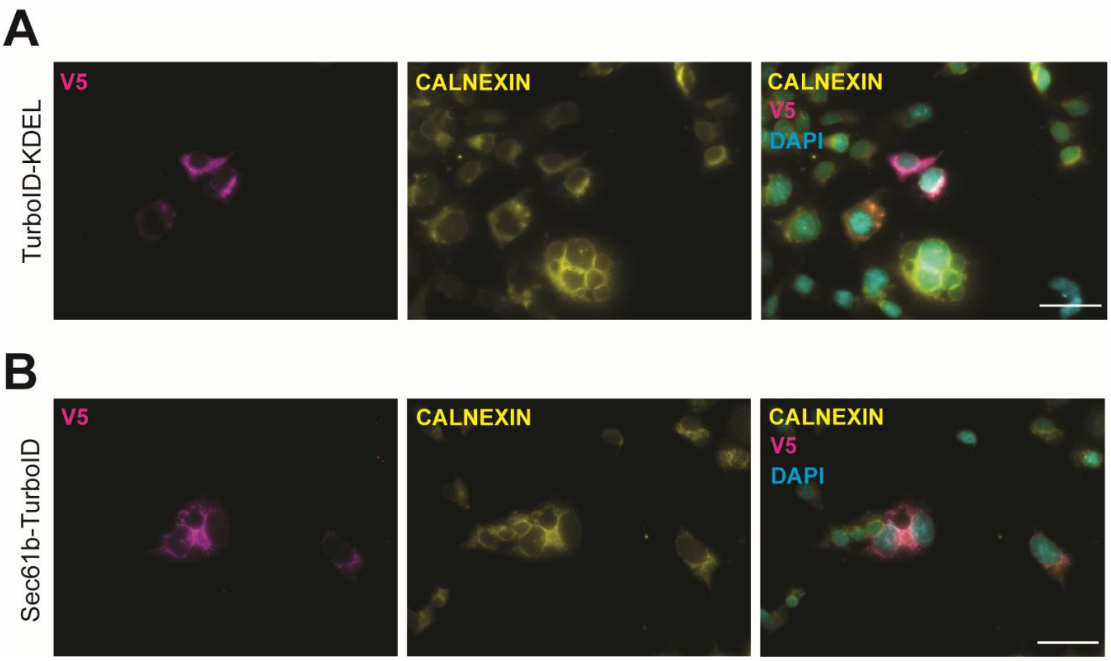

***Figure 2* – TurboID-KDEL and Sec61b-TurboID colocalise with the ER-resident protein calnexin.** Cos-7 cells were transfected with pMX-IgK-TurboID-V5-KDEL (A) or pcDNA5-Sec61b-TurboID (B). 24h after transfection, cells were fixed and stained for DAPI (cyan), V5 (magenta) and calnexin (yellow). Representative images from one (B) or two (A) independent experiments. Scale bars, 40 µm.

Next, to observe the range of biotinylated proteins present inside transfected cells treated with biotin, I run cell lysates on SDS-PAGE for a Western Blot. The same was performed with conditioned medium from these cells.

Although COS-7 cells were a good choice to clearly see the ER by IF, we observed very low transfection rates for these cells using PEI. As HEK-293T cells are much easier to transfect with PEI, this cell line was used for the next set of experiments.

HEK-293T cells were transfected with either pcDNA5-Sec61b-V5-TurboID or pMX-IgK-TurboID-V5-KDEL and treated with biotin for one hour the next day. Cells were then left to secrete protein into new medium for twenty-four hours. Medium and lysate samples were collected and run on an SDS-PAGE. Proteins were transferred to a nitrocellulose membrane and blotted with a streptavidin conjugate. A range of biotinylated proteins with different molecular weights appear on lysates from cells transfected with pcDNA5-Sec61b-V5-TurboID and treated with biotin. Cells transfected with pMX-IgK-TurboID-V5-KDEL show fewer biotinylated proteins throughout a similar range of molecular weights (*Figure 4A*). Conditioned media from transfected cells treated with biotin also present a range of biotinylated proteins (*Figure 4B*), and similarly to what was observed for cell lysates, cells transfected with pMX-

IgK-TurboID-V5-KDEL secrete less biotinylated proteins than the ones transfected with pcDNA5-Sec61b-V5-TurboID. This difference in the amount of biotinylated proteins probably relies mostly on the fact that TurboID expression is under the control of different promoters on the two tested plasmids (see *Discussion 4.1.*).

Collectively, these sets of experiments show that, upon biotin addition, ER-retained TurboID biotinylates proteins in transfected cells, and that biotinylated proteins are being secreted into culture medium.

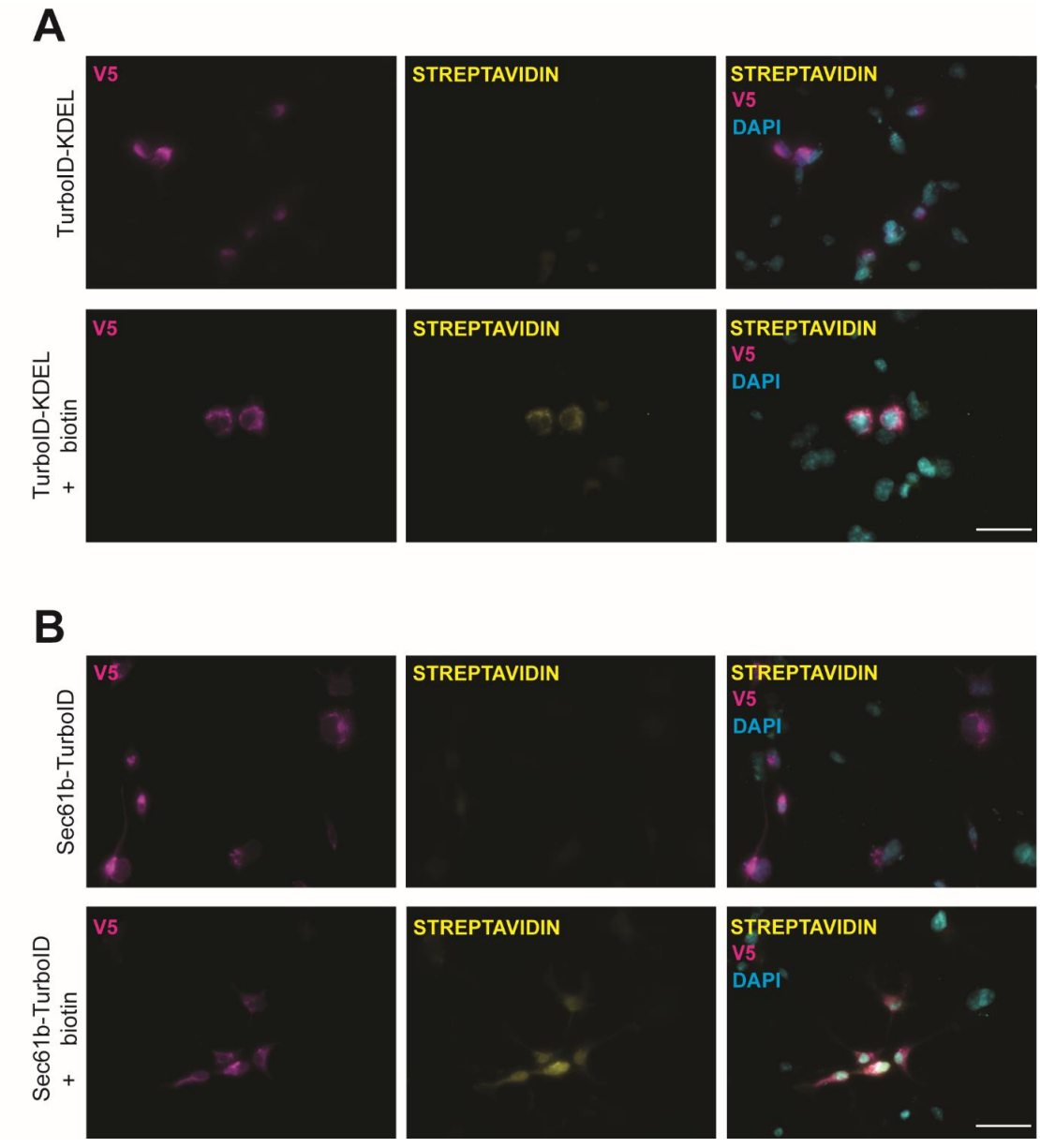

***Figure 3* – TurboID-KDEL and Sec61b-TurboID biotinylate proteins upon biotin addition.** Cos-7 cells were transfected with either pMX-IgK-TurboID-V5-KDEL (A) or pcDNA5-Sec61b-TurboID (B). 24h after transfection, cells were treated with 100 µM of biotin for 1 hour, fixed, and stained with DAPI (cyan), anti-V5 (magenta), and streptavidin-Texas Red (yellow). Cells

that were not treated with biotin were used as a negative control. Representative images from one (A) or three (B) independent experiments. Scale bars, 40 μm.

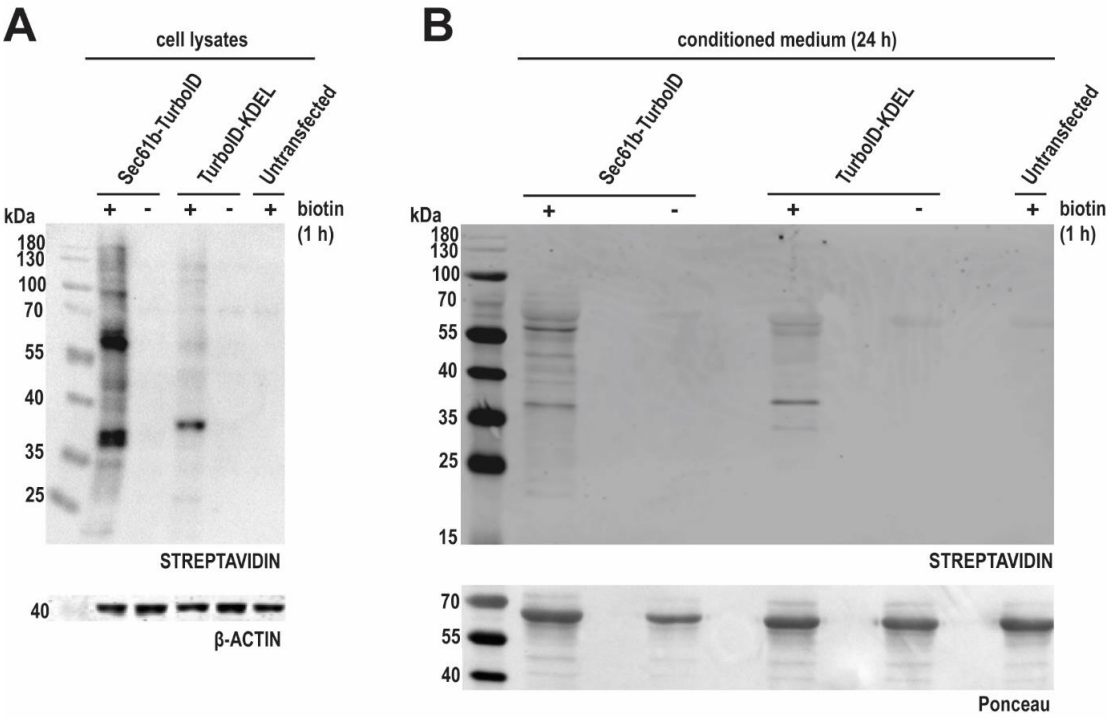

***Figure 4* – Upon biotin addition, Sec61b-TurboID and TurboID-KDEL biotinylate several proteins that are secreted into the medium.** HEK293T cells were transfected with either pcDNA5-Sec61b-TurboID or pMX-IgK-TurboID-V5-KDEL. 24h after transfection, cells were treated with 100 μM of biotin for 1 hour and left to secrete protein into new medium for 24 hours. Lysates (A) and media (B) were collected. Protein was extracted from lysates, and media samples were concentrated. Samples were run on an SDS-PAGE, transferred to a nitrocellulose membrane, and blotted with streptavidin-HRP (A) or streptavidin 647 (B). Transfected cells that were not treated with biotin, and untransfected cells treated with biotin were used as negative controls. β-actin and Ponceau staining were used as a loading control for lysate and medium samples, respectively. Representative images from two independent experiments.

3.2. Longer biotin pulses and chases allow the collection of more biotinylated proteins

As the amount of biotinylated proteins collected from conditioned media was relatively low (*Figure 4B*), especially using pMX-IgK-TurboID-V5-KDEL. I tested different biotinylation and chase conditions in an attempt to maximise the amount and/or number of biotinylated proteins. To have a closer approximation to what would happen in primary astrocytes, these experiments were performed on an astrocyte-like cell line (C8-D1A). Cells were transfected using lipofectamine to ensure higher transfection rates.

Firstly, to assess if different incubation conditions with biotin could maximise the amount of biotinylated proteins in cells transfected with pMX-IgK-TurboID-V5-KDEL, different conditions were tested.

Kim and colleagues incubate cells expressing Sec61b-TurboID for up to 4 hours, seeing a continuous increase in protein biotinylation inside transfected cells cells throughout the four hours.[67] I wondered how far we could further increase incubation time with biotin before reaching saturation.

Using BioID2-KDEL, Liu and colleagues applied two 6-hour pulses before chasing proteins into the medium.[60] With this in mind, I also tested two or three smaller biotin pulses.

Thus, the conditions used for this experiment were: 1-hour biotin pulse (used in previous experiments); two and three 1 hour pulses; one and two 6 hour pulses; and a long 16-hour pulse.

Figure 5 shows an increase in the amount of biotinylated proteins inside the cells when the incubation time with biotin increases. Remarkably, a very big boost in biotinylation is observed upon two 6 hour- or one 16 hour-pulse(s) with biotin.

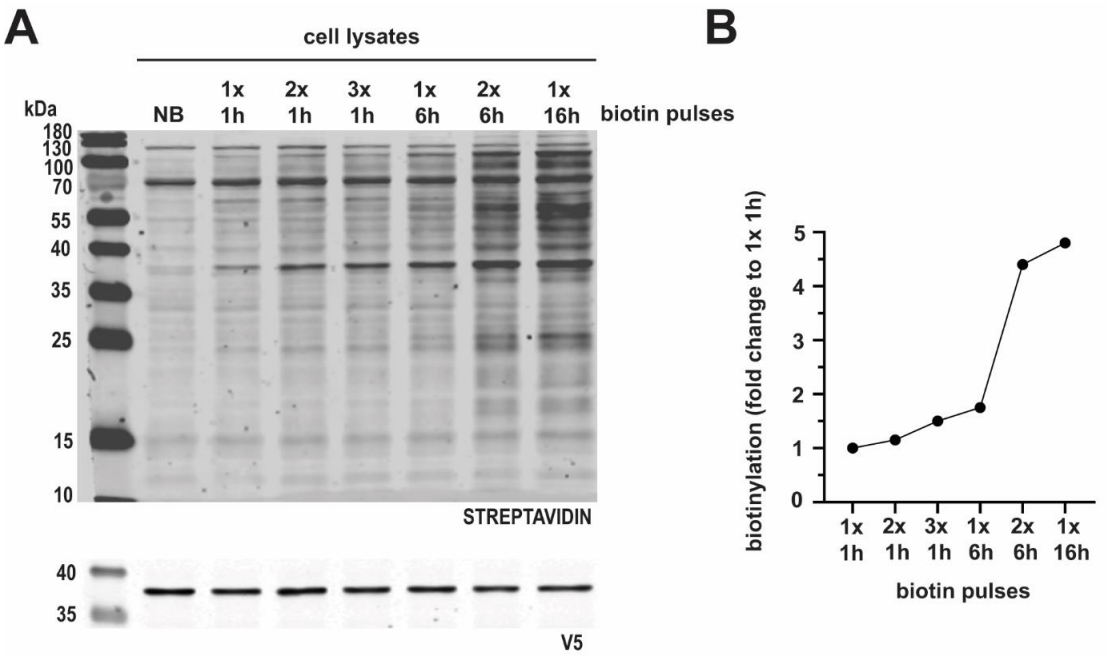

***Figure 5* – Longer incubation times with biotin result in more biotinylated proteins inside cells.** C8-D1A cells were transfected with pMX-IgK-TurboID-V5-KDEL. 24h after transfection, cells underwent pulses of 100 µM biotin: either one, two or three 1-hour pulses; either one or two 6-hour pulses; or a long 16-hour pulse. Lysates were collected and protein extracted. Samples were run on an SDS-PAGE, transferred to a membrane, and blotted with streptavidin-647 (A). Transfected cells that were not treated with biotin as a negative control. Quantification of the streptavidin signal is plotted in (B). Streptavidin signal was normalised with V5 signal, and results shown as a fold change of the of the 1-hour pulse condition. (N=1)

Next, I wanted to assess if increasing chase times up to three days would significantly increase the amount of biotinylated proteins collected from conditioned medium. C8-D1A cells were plated in several 6-well plate wells, transfected with pMX-IgK-TurboID-KDEL and incubated with biotin overnight (to maximise biotinylation). Three chase times were tested: 24, 48 and 72 hours. Additionally, a lysate collected right after 18 hours of incubation with biotin was used as a positive loading control (*Figure 6*). Medium from the same cells was also collected and run on the gel to check the amount of biotinylated proteins secreted during biotin incubation and, therefore, "lost" for our analysis. As a negative control, medium from cells that were not treated with biotin was run on the gel. Finally, for comparison with previous experiments (*Figure 4*), medium from cells that underwent a 1-hour biotin pulse followed by a 24-hour chase was used.

Increasing the chase time from 24 hours to 72 hours did not result in a significant increase in collected biotinylated proteins, implying that the majority of labelled proteins were trafficked and secreted into the media relatively quickly (*Figure*

4). An interesting observation is that right after the long (18-hour) biotin incubation, there are more biotinylated proteins in the medium than on the next 72 hours.

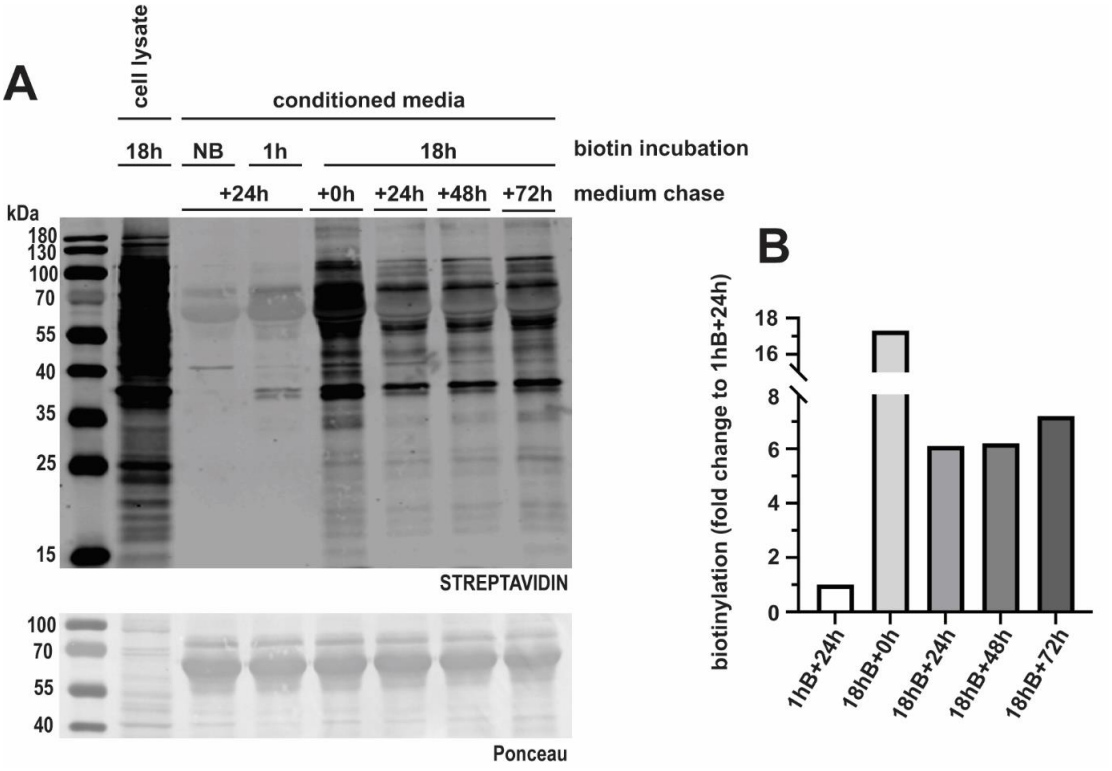

***Figure 6* – A long incubation with biotin followed by long chases can boost the amount of biotinylated proteins secreted into the medium.** C8D1A cells were transfected with pMX-IgK-TurboID-V5-KDEL. The day after transfection, cells underwent a long 18-hour pulse of 100 µM biotin, after which lysates and medium were collected. Other sets of cells were left to secrete protein into the medium for either 24, 48 or 72 hours after this pulse. Conditioned media were collected. Other cells were used to collect the conditioned medium from a no-biotin (negative) control and the previously used condition of a 1-hour pulse followed by a 24-hour chase (condition used on previous experiments – *Figure 4*). Protein was extracted from lysates, and media samples were concentrated. Samples were run on an SDS-PAGE, transferred to a membrane, and blotted with streptavidin-647 (A). Quantification of the streptavidin signal is plotted in (B). Streptavidin signal was normalised with Ponceau staining, and results are shown as a fold change of the 1-hour pulse and 24-hour chase condition. (N=1)

3.3. Applying the system to primary astrocytes

After validating and optimising the system on cell lines, it was tested in mouse primary astrocytes.

Primary astrocyte cultures from the cortex of P1 mice are well established in the host Laboratory and routinely show around 80% purity (data not shown; João Guimarães). Due to these small levels of contamination with other cell types, TurboID-KDEL and Sec61b-TurboID expression will be under the control of an astrocyte-specific promoter (gfa2).[76]

Since transfecting primary astrocytes is difficult and low-efficient[77] and since transfected cells lose plasmid upon cell division, DNA was delivered to astrocytes using lentiviral vectors (LVs), which have been proven efficient in these cells in the past.[78]

Lentiviral vectors have been genetically modified from the human immunodeficiency virus 1 (HIV-1) to deliver genetic material to cells. The HIV-1 virus carries genomic RNA, a reverse transcriptase and an integrase. Upon infection, the RNA is converted into proviral double-stranded DNA that is integrated into the host's genome. Host's cell machinery will then transcribe the viral machinery and genomic RNA, leading to the production of new viruses.

Lentiviral vectors are produced in a way that only allows transfer DNA integration in the host's genome, but not viral replication. This is done by splitting the viral genome into different plasmids (a transfer plasmid with the transgene, and plasmids expressing the viral machinery). Cultured cells are transfected with these plasmids and, inside transfected cells, viral particles are formed with genomic RNA only expressing the desired transgene, so the virus does not have the ability to replicate further.

These viral vectors are collected and can be used to deliver the specific transgene to cells by allowing genome integration of the transfer DNA. Additionally, in lentiviral vectors, HIV-1 envelope proteins that only bind immune cells are replaced by VSV-G, which binds an ubiquitous membrane component, allowing the vectors to transduce a very wide variety of cells.[79]

Transfer plasmids used for LVs production were: pFUGW-gfa2-IgK-TurboID-HA-KDEL and pFUGW-gfa2-Sec61b-V5-TurboID (plasmid maps on *Supplementary information*).

3.3.1. TurboID-KDEL and Sec61b-TurboID can biotinylate protein in primary astrocytes

Primary astrocytes from the cortex of P1 mice were transduced with a multiplicity of infection (MOI) of 10 with lentiviral vectors carrying either pFUGW-IgK-TurboID-HA-KDEL or pFUGW-Sec61b-V5-TurboID. Staining with antibodies for the epitope tags and streptavidin shows that transduced astrocytes express TurboID and that it is active (*Figure 7*). Although transduction rates were not high, these preliminary results in primary astrocytes show that the system can most likely be used on these cells.

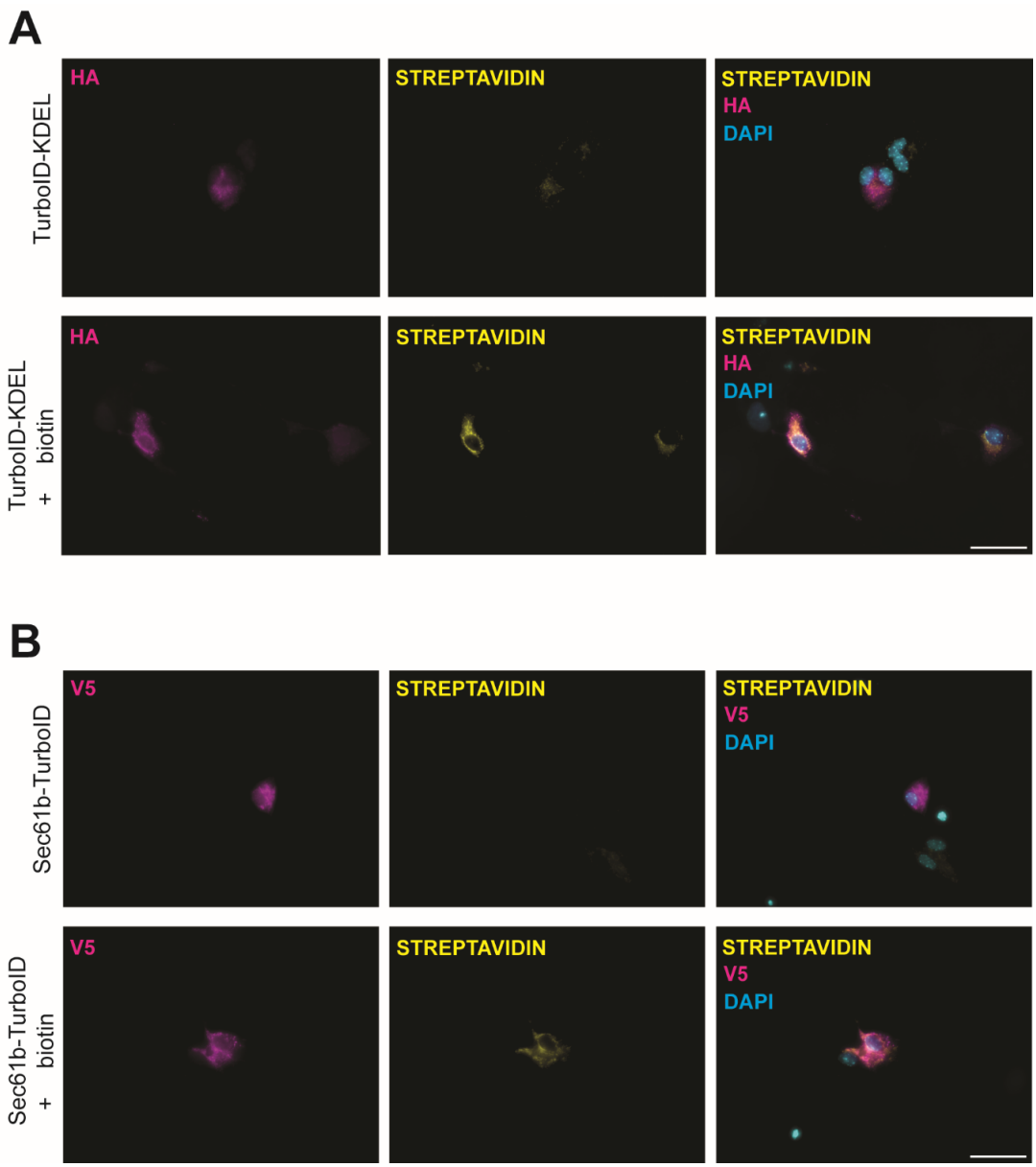

***Figure 7* – TurboID-KDEL and Sec61b-TurboID biotinylate proteins in primary astrocytes.** Primary astrocytes were transduced with lentiviral vectors carrying either pFUGW-IgK-TurboID-HA-KDEL (A) or pFUGW-Sec61b-V5-TurboID (B). One week after transduction, astrocytes

were treated with 100 μM of biotin for 1 hour, fixed and stained with DAPI (cyan), either anti-HA (A) or anti-V5 (B) (magenta), and streptavidin-647 (yellow). Cells that were not treated with biotin were used as a negative control. Scale bars, 40 μm. (N=1)

4. Discussion

Astrocytes are known to regulate synapse formation through cell surface adhesion proteins and secreted proteins.[23] However, many of these factors are yet to be identified, especially the ones involved in inhibitory synapse assembly and maturation (Table 1).

With the goal of identifying astrocyte-secreted factors that could be involved in inhibitory or excitatory synapse formation, I validated a protein biotinylation system to unravel the astrocyte-specific secretome. To do this, the biotin ligase TurboID can be directed to the ER of cultured astrocytes and specifically biotinylate proteins in the ER lumen. Since most secreted proteins transit through the ER, biotinylated proteins can then be collected from the medium, easily purified and identified by mass spectrometry.[60,67] From the determined astrocyte secretome, candidate proteins can be selected to be tested for synaptogenic potential.

4.1. System validation in cultured cell lines

To validate the system, I started by testing two constructs expressing TurboID linked to two different ER retention sequences – KDEL and Sec61b – on commonly used cell lines. While TurboID-KDEL will be retained "freely" inside in the lumen of the ER, Sec61b-TurboID will be anchored to the ER membrane in such a way that TurboID is directed to the ER lumen.[67] By using both these systems, we might biotinylate two different ER protein pools, ensuring a rather complete survey of the astrocyte secretome.

To confirm that TurboID-KDEL and Sec61b-TurboID are in the ER, I used the COS-7 cell line, very flat cells which are advantageous to clearly see this organelle. By transfecting COS-7 cells with pMX-IgK-TurboID-V5-KDEL and pcDNA5-Sec61b-V5-TurboID, I confirmed by immunofluorescence that both TurboID-KDEL and Sec61b-TurboID are retained in the ER (*Figure 2*) and that TurboID is active in transfected cells (*Figure 3*).

In these first experiments on COS-7 cells, transfection rates with PEI were relatively low (around 25% with 1 µg PEI; data not shown). Although the number of transfected cells was more than enough to perform the validation experiments by IF, low transfection rates could be a problem for the Western Blot validation: few transfected cells would result in few biotinylated proteins in both lysates and conditioned medium samples for analysis. With this in mind, and knowing that HEK-293T cells, despite not being so suitable to see the ER clearly, show higher transfection

rates (more than 50% with 0.5 µg PEI; data not shown), I used this cell line for the first validations by Western Blot.

By Western Blot, by transfecting HEK-293Tcells with the same plasmids, I confirmed that a range of proteins were being biotinylated inside transfected cells (*Figure 4B*) and that a range of biotinylated proteins were secreted by these cells and could be successfully collected (*Figure 4B*).

Differences were observed between the two plasmids, both in the amount of proteins biotinylated inside the cells and secreted into the medium (*Figure 4*). This difference is most likely due to the different promoters present in the pMX-IgK-TurboID-V5-KDEL and pcDNA5-Sec61b-V5-TurboID plasmids. While the pMX has long terminal repeat (LTR) sequences as a promoter, the pcDNA5 has a cytomegalovirus (CMV) promoter. The last has been proven to be a very strong promoter,[80] which goes accordingly with the results obtained: a stronger promoter driving the expression of Sec61b-TurboID will result in more enzyme being expressed and, consequently, more biotinylated proteins being collected for WB analysis.

Another important detail of these WB experiments is that cells, which are usually cultured in DMEM with 10% FBS, were left to secrete protein into medium with low FBS (0.1%). This was done since, even with size fractionation using a gel, a higher FBS concentration could result in low-abundance proteins being masked. It is important to state that these cells are in nutrient deprivation and, therefore, not as healthy as they would be in complete medium. Although twenty-four hours in these conditions did not seem to significantly affect HEK-293T cells in terms of morphology or growth (data not shown), cells should not be left for long in serum deprivation. Nonetheless, when we apply the system to primary astrocytes, low-serum conditions are only needed for a first validation by Western Blot. For the mass spectrometry analysis, as biotinylated proteins will be isolated using streptavidin beads, FBS contamination should almost disappear, and therefore, normal culturing conditions can be used.

4.2. Maximising biotinylation by increasing biotin incubation and chase times

Next, different biotin incubations and chase conditions were tested on the astrocyte-like cell line C8-D1A.[81] Since these cells show very low transfection rates using PEI (around 10%), experiments on C8-D1A cells were performed using lipofectamine as a transfection reagent (transfection rate around 60%).

These experiments were only performed once. Therefore, although the results are qualitatively in line with what would be expected, they are only preliminary and would require a greater number of repetitions for proper quantification.

When cells were incubated with biotin for longer, a great increase in the amount of biotinylated proteins inside the cells was observed (*Figure 5*). Therefore, in following experiments, cells were incubated with biotin overnight.

Regarding the experiment where chase times were increased (*Figure 6*), only a small increase was observed in the amount of biotinylated proteins that could be collected after 72 hours of secretion compared to the previously tested 24 hours. This suggests that a 24-hour chase might be enough for most proteins to be secreted, and to use in following experiments.

Nonetheless, I noticed that right after the overnight biotin incubation, there were more biotinylated proteins in the medium than in the next 72 hours. This might mean that a lot of the proteins that were biotinylated by TurboID might be secreted during those initial hours. Therefore, doing several shorter pulses and collecting medium between each pulse could be a good approach to avoid losing biotinylated secreted proteins.

Another possible explanation could be that this large amount of biotinylated proteins during incubation with biotin could partially be due to some secretion of TurboID-KDEL (reported by Kim et al., 2021).[67] However, considering that there is no ATP in the cell culture medium, even if secreted, the enzyme would most likely not be active in the in the medium.

4.3. Applying the system to primary astrocytes

Although there has been some debate about how well cultured astrocytes represent the *in vivo* situation,[82] primary astrocyte cultures, like the ones employed in this study, have been extensively used to identify secreted synaptogenic factors,[26,33] as well as studying astrocyte function and their involvement in various disorders.[83]

Therefore, we combined the use of cultures with TurboID to facilitate secretome identification. Although other biotinylating enzymes, like HRP and APEX2, were considered for this project, we observed that H_2O_2 is very toxic to mouse primary astrocytes (data not shown; João Guimarães) and therefore decided to use TurboID for this study.

TurboID has been employed to study the secretome both *in vitro* and *in vivo*.[60,67] In their study on endothelial cells, Liu and colleagues state that the *in vitro* approach on cultured cells yielded much more proteins than the *in vivo* one, that involved collecting proteins from mouse serum.[60] Moreover, determining cell-specific

secretome from brain cells *in vivo* would involve the collection of cerebrospinal fluid rather than serum, which is a much more difficult and stress-inducing procedure.[84] Additionally, since biotinylation, *in vivo*, is induced by dietary supplementation, biotin concentration can never reach the amounts used in cultured cells.

A first experiment using lentiviral vectors to deliver TurboID-KDEL and Sec61b-TurboID to primary astrocytes shows specific biotinylation in transduced cells (*Figure 7*). Moreover, although a calnexin staining was not performed in these cells, both HA and V5 stainings show an intracellular distribution similar to the ER staining observed for other cell types (*Figure 2*). A big limitation observed in this experiment was that less than 40% of the cells express TurboID (data not shown) and that expression levels appear to be relatively low. To overcome this problem, several approaches could be taken, such as concentrating the lentiviral vectors to be able to use higher MOIs. This could be done, for example, by ultracentrifugation on precipitation.[85] Another option would be performing the transduction using spin inoculation or using reagents that could facilitate transduction. Polybrene, one of the most used transduction-facilitating reagents, was tested on our cultures and showed very high toxicity towards mouse primary astrocytes (data not shown). However, other reagents, like protamine sulphate[86] or LentiBOOST[87] could be tested. As a last resource, since a culturing protocol for rat primary astrocytes has also been established at the host laboratory, rat astrocytes could be used instead of mouse ones. These astrocytes are usually more tolerant to various experimental conditions and more proliferative, and are not as sensitive to polybrene (data not shown; Simone Bessa). However, there were reasons that led us to choose mouse astrocytes to begin with. Although mouse and rat genomes have high homology,[88] we will perform further *in vivo* studies, in a murine model, of proteins of interest in regard to their synaptogenic potential and involvement in disease.

4.4. Possible limitations of the system

One possible system limitation would be that, when analysing the secretome, since TurboID biotinylates proteins in lysine residues, there could be a bias towards proteins with high lysine content. Although Liu and colleagues compared the lysine content of the secretome they obtained using proximity biotinylation with another data set with the secretome from the same cell type (endothelial cells) and concluded that both sets had similar lysine contents,[60] it would be interesting to analyse transcriptome data to get an idea of lysine usage in astrocytes.

Another limitation is that TurboID, by only biotinylating proteins in the ER lumen, will miss some proteins that are secreted by unconventional modes. Although

most secreted proteins transit through the ER, proteins that are secreted through Type I, II and III unconventional protein secretion do not,[89] and therefore will not appear in any secretome identified using ER-retained TurboID.

5. Conclusions and Future Perspectives

Overall, I validated two different constructs – TurboID-KDEL and Sec61b-TurboID – that could be used to label proteins in the secretory pathway of primary astrocytes. Proteins can then be collected from medium, quickly purified and identified by mass spectrometry to obtain the astrocyte secretome.

I confirmed that both TurboID-KDEL and Sec61b-TurboID are active and retained in the ER. Proteins biotinylated by TurboID are secreted and can be collected from the culture medium.

Additionally, I confirmed that lentiviral vectors can successfully deliver these constructs to primary mouse astrocytes and that TurboID is active in astrocytes expressing these constructs.

In the future, this system should be applied to primary mouse astrocytes to determine their secretome. To do this, I would start by increasing the amount of cells expressing the constructs by concentrating the lentiviral vectors and increasing the multiplicity of infection used. If neither this, or using reagents that enhance infectivity worked, I would test the system on rat astrocytes, which may be more permissive.

After having 50% or more cells expressing the constructs to ensure that I would be able to collect enough secreted biotinylated proteins for MS analysis, I would perform Western Blot to confirm that proteins biotinylated inside cells were being secreted and could be collected from the culture medium. After this, biotinylated proteins collected from the medium could be purified using streptavidin pull-down. Proper purification can be confirmed by running the flow through, washes and eluted proteins on an SDS-PAGE, transferring proteins to a membrane and blotting with streptavidin. The system could then be expanded: cell cultures could be scaled up, then transduced, treated with biotin, and medium could be collected for LC-MS/MS analysis.[90] By LC-MS/MS, we would identify the mouse astrocyte secretome.

The list of proteins obtained by LC-MS/MS should be thoroughly analysed using literature, bioinformatic tools, databases, and genomic-wide association studies,[91,92] in order to select proteins that make sense in the context of the mouse secretome, synapse assembly, and neurodevelopmental disorders.

The synaptogenic potential of selected proteins can be assessed using neuronal primary cultures. After adding purified protein to the cells, the number of excitatory and inhibitory synapses can be quantified by counting the number of colocalising pre- and post-synaptic immunomarkers.[48]

Moreover, proteins that are shown to be synaptogenic *in vitro* can be tested *in vivo*. Each protein of interest can be knocked-out in astrocytes using the CRISPR-Cas9 system. Structural and functional studies of synapses can then be performed in these mice, using immunofluorescence for synaptic markers[93] and electrophysiology to record post-synaptic currents. Additionally, behavioural tests can be performed to assess a possibly disordered phenotype.

6. References

1. Splittgerber, R. *Snell's Clinical Neuroanatomy*. (2019).
2. Allen, N. J. & Lyons, D. A. Glia as architects of central nervous system formation and function. *Science* vol. 362 181–185 Preprint at https://doi.org/10.1126/science.aat0473 (2018).
3. Sperelakis, N. *Cell Physiology Sourcebook Essentials of Membrane Biophysics*. (2012).
4. Südhof, T. C. Towards an Understanding of Synapse Formation. *Neuron* vol. 100 276–293 Preprint at https://doi.org/10.1016/j.neuron.2018.09.040 (2018).
5. Südhof, T. C. The cell biology of synapse formation. *Journal of Cell Biology* vol. 220 Preprint at https://doi.org/10.1083/jcb.202103052 (2021).
6. Brill, J. & Huguenard, J. R. Sequential changes in AMPA receptor targeting in the developing neocortical excitatory circuit. *Journal of Neuroscience* **28**, 13918–13928 (2008).
7. Favuzzi, E. & Rico, B. Molecular diversity underlying cortical excitatory and inhibitory synapse development. *Current Opinion in Neurobiology* vol. 53 8–15 Preprint at https://doi.org/10.1016/j.conb.2018.03.011 (2018).
8. Kumar, S. S., Bacci, A., Kharazia, V. & Huguenard, J. R. *A Developmental Switch of AMPA Receptor Subunits in Neocortical Pyramidal Neurons*. (2002).
9. Roberts, A. C. *et al.* Downregulation of NR3A-Containing NMDARs Is Required for Synapse Maturation and Memory Consolidation. *Neuron* **63**, 342–356 (2009).
10. Sohal, V. S. & Rubenstein, J. L. R. Excitation-inhibition balance as a framework for investigating mechanisms in neuropsychiatric disorders. *Mol Psychiatry* **24**, 1248–1257 (2019).
11. Rubenstein, J. L. R. & Merzenich, M. M. Model of autism: increased ratio of excitation/ inhibition in key neural systems. doi:10.1046/j.1601-183X.2003.00037.x.
12. Bozzi, Y., Casarosa, S. & Caleo, M. Epilepsy as a neurodevelopmental disorder. *Frontiers in Psychiatry* vol. 3 Preprint at https://doi.org/10.3389/fpsyt.2012.00019 (2012).
13. Li, W. Excitation and Inhibition Imbalance in Rett Syndrome. *Frontiers in Neuroscience* vol. 16 Preprint at https://doi.org/10.3389/fnins.2022.825063 (2022).

14. Shao, L. R. *et al.* Increased propensity for infantile spasms and altered neocortical excitation-inhibition balance in a mouse model of down syndrome carrying human chromosome 21. *Neurobiol Dis* **184**, (2023).
15. Liu, Y. *et al.* A Selective Review of the Excitatory-Inhibitory Imbalance in Schizophrenia: Underlying Biology, Genetics, Microcircuits, and Symptoms. *Frontiers in Cell and Developmental Biology* vol. 9 Preprint at https://doi.org/10.3389/fcell.2021.664535 (2021).
16. Mamiya, P. C., Arnett, A. B. & Stein, M. A. Precision medicine care in ADHD: The case for neural excitation and inhibition. *Brain Sci* **11**, 1–12 (2021).
17. Holt, M. G. Astrocyte heterogeneity and interactions with local neural circuits. *Essays in Biochemistry* vol. 67 93–106 Preprint at https://doi.org/10.1042/EBC20220136 (2023).
18. Barres, B. A. The Mystery and Magic of Glia: A Perspective on Their Roles in Health and Disease. *Neuron* vol. 60 430–440 Preprint at https://doi.org/10.1016/j.neuron.2008.10.013 (2008).
19. Volterra, A. & Meldolesi, J. Astrocytes, from brain glue to communication elements: The revolution continues. *Nature Reviews Neuroscience* vol. 6 626–640 Preprint at https://doi.org/10.1038/nrn1722 (2005).
20. Tan, C. X., Burrus Lane, C. J. & Eroglu, C. Role of astrocytes in synapse formation and maturation. in *Current Topics in Developmental Biology* vol. 142 371–407 (Academic Press Inc., 2021).
21. Volterra, A., Liaudet, N. & Savtchouk, I. Astrocyte Ca2+ signalling: An unexpected complexity. *Nature Reviews Neuroscience* vol. 15 327–335 Preprint at https://doi.org/10.1038/nrn3725 (2014).
22. D'Antoni, S. *et al.* Metabotropic glutamate receptors in glial cells. *Neurochemical Research* vol. 33 2436–2443 Preprint at https://doi.org/10.1007/s11064-008-9694-9 (2008).
23. Allen, N. J. & Eroglu, C. Cell Biology of Astrocyte-Synapse Interactions. *Neuron* vol. 96 697–708 Preprint at https://doi.org/10.1016/j.neuron.2017.09.056 (2017).
24. Sofroniew, M. V. Astrogliosis. *Cold Spring Harb Perspect Biol* **7**, (2015).
25. Liddelow, S. A. *et al.* Neurotoxic reactive astrocytes are induced by activated microglia. *Nature* **541**, 481–487 (2017).
26. Ullian, E. M., Harris, B. T., Wu, A., Chan, J. R. & Barres, B. A. Schwann cells and astrocytes induce synapse formation by spinal motor neurons in culture. *Molecular and Cellular Neuroscience* **25**, 241–251 (2004).

27. Pfrieger, F. W. & Barres, B. A. Synaptic Efficacy Enhanced by Glial Cells in Vitro. *Science (1979)* **277**, 1684–1687 (1997).
28. Chung, W. S., Allen, N. J. & Eroglu, C. Astrocytes control synapse formation, function, and elimination. *Cold Spring Harb Perspect Biol* **7**, (2015).
29. Molofsky, A. V. *et al.* Astrocyte-encoded positional cues maintain sensorimotor circuit integrity. *Nature* **509**, 189–194 (2014).
30. Garrett, A. M. & Weiner, J. A. Control of CNS synapse development by γ-protocadherin-mediated astrocyte-neuron contact. *Journal of Neuroscience* **29**, 11723–11731 (2009).
31. Carmona, M. A., Murai, K. K., Wang, L., Roberts, A. J. & Pasquale, E. B. *Glial Ephrin-A3 Regulates Hippocampal Dendritic Spine Morphology and Glutamate Transport*. www.pnas.org/cgi/content/full/.
32. Stogsdill, J. A. *et al.* Astrocytic neuroligins control astrocyte morphogenesis and synaptogenesis. *Nature* **551**, 192–197 (2017).
33. Christopherson, K. S. *et al.* Thrombospondins are astrocyte-secreted proteins that promote CNS synaptogenesis. *Cell* **120**, 421–433 (2005).
34. Kucukdereli, H. *et al.* Control of excitatory CNS synaptogenesis by astrocyte-secreted proteins hevin and SPARC. *Proc Natl Acad Sci U S A* **108**, (2011).
35. Goritz, C., Mauch, D. H. & Pfrieger, F. W. Multiple mechanisms mediate cholesterol-induced synaptogenesis in a CNS neuron. *Molecular and Cellular Neuroscience* **29**, 190–201 (2005).
36. Mauch, D. H. *et al.* CNS synaptogenesis promoted by glia-derived cholesterol. *Science (1979)* **294**, 1354–1357 (2001).
37. Crawford, D. C., Jiang, X., Taylor, A. & Mennerick, S. Astrocyte-derived thrombospondins mediate the development of hippocampal presynaptic plasticity in vitro. *Journal of Neuroscience* **32**, 13100–13110 (2012).
38. Blondel, O. *et al. A Glia-Derived Signal Regulating Neuronal Differentiation*. (2000).
39. Hennekinne, L., Colasse, S., Triller, A. & Renner, M. Differential control of thrombospondin over synaptic glycine and AMPA receptors in spinal cord neurons. *Journal of Neuroscience* **33**, 11432–11439 (2013).
40. Allen, N. J. *et al.* Astrocyte glypicans 4 and 6 promote formation of excitatory synapses via GluA1 AMPA receptors. *Nature* **486**, 410–414 (2012).
41. Beattie, E. C. , *et al.* Control of synaptic strength by glial TNFα. *Science (1979)* **295**, 2282–2285 (2002).

42. Stellwagen, D., Beattie, E. C., Seo, J. Y. & Malenka, R. C. Differential regulation of AMPA receptor and GABA receptor trafficking by tumor necrosis factor-α. *Journal of Neuroscience* **25**, 3219–3228 (2005).
43. Blanco-Suarez, E., Liu, T. F., Kopelevich, A. & Allen, N. J. Astrocyte-Secreted Chordin-like 1 Drives Synapse Maturation and Limits Plasticity by Increasing Synaptic GluA2 AMPA Receptors. *Neuron* **100**, 1116-1132.e13 (2018).
44. Fossati, G. *et al.* Pentraxin 3 regulates synaptic function by inducing AMPA receptor clustering via ECM remodeling and β1-integrin. *EMBO J* **38**, (2019).
45. Elmariah, S. B., Oh, E. J., Hughes, E. G. & Balice-Gordon, R. J. Astrocytes regulate inhibitory synapse formation via Trk-mediated modulation of postsynaptic GABAA receptors. *Journal of Neuroscience* **25**, 3638–3650 (2005).
46. Takano, T. *et al.* Chemico-genetic discovery of astrocytic control of inhibition in vivo. *Nature* **588**, 296–302 (2020).
47. Mclean Bolton, M., Pittman, A. J. & Lo, D. C. *Brain-Derived Neurotrophic Factor Differentially Regulates Excitatory and Inhibitory Synaptic Transmission in Hippocampal Cultures*. (2000).
48. Irala, D. *et al.* Astrocyte-Secreted Neurocan Controls Inhibitory Synapse Formation and Function 2. doi:10.1101/2023.04.03.535448.
49. Diniz, L. P., Matias, I. C. P., Garcia, M. N. & Gomes, F. C. A. Astrocytic control of neural circuit formation: Highlights on TGF-beta signaling. *Neurochemistry International* vol. 78 18–27 Preprint at https://doi.org/10.1016/j.neuint.2014.07.008 (2014).
50. Fuentes-Medel, Y. *et al.* Integration of a retrograde signal during synapse formation by glia-secreted TGF-β ligand. *Current Biology* **22**, 1831–1838 (2012).
51. Lesch, K. P. *et al.* Molecular genetics of adult ADHD: Converging evidence from genome-wide association and extended pedigree linkage studies. *J Neural Transm* **115**, 1573–1585 (2008).
52. Calboli, F. C. F. *et al.* A genome-wide association study of neuroticism in a population-based sample. *PLoS One* **5**, (2010).
53. Garcia, O., Torres, M., Helguera, P., Coskun, P. & Busciglio, J. A role for thrombospondin-1 deficits in astrocyte-mediated spine and synaptic pathology in down's syndrome. *PLoS One* **5**, (2010).
54. Ballas, N., Lioy, D. T., Grunseich, C. & Mandel, G. Non-cell autonomous influence of MeCP2-deficient glia on neuronal dendritic morphology. *Nat Neurosci* **12**, 311–317 (2009).

55. Jacobs, S. & Doering, L. C. Astrocytes prevent abnormal neuronal development in the fragile X mouse. *Journal of Neuroscience* **30**, 4508–4514 (2010).
56. Diniz, L. P. *et al.* Astrocyte transforming growth factor beta 1 promotes inhibitory synapse formation via CaM kinase II signaling. *Glia* **62**, 1917–1931 (2014).
57. Diniz, L. P. *et al.* Astrocyte-induced synaptogenesis is mediated by transforming growth factor β signaling through modulation of d-serine levels in cerebral cortex neurons. *Journal of Biological Chemistry* **287**, 41432–41445 (2012).
58. Piersma, S. R. *et al.* Workflow comparison for label-free, quantitative secretome proteomics for cancer biomarker discovery: Method evaluation, differential analysis, and verification in serum. *J Proteome Res* **9**, 1913–1922 (2010).
59. Brown, K. J. *et al.* Advances in the proteomic investigation of the cell secretome. *Expert Review of Proteomics* vol. 9 337–345 Preprint at https://doi.org/10.1586/epr.12.21 (2012).
60. Liu, J. *et al.* The secretome mouse provides a genetic platform to delineate tissue-specific in vivo secretion. doi:10.1073/pnas.2005134118/-/DCSupplemental.
61. Kang, M. G. & Rhee, H. W. Molecular Spatiomics by Proximity Labeling. *Acc Chem Res* (2022) doi:10.1021/acs.accounts.2c00061.
62. Bosch, J. A., Chen, C.-L. & Perrimon, N. Proximity-dependent labeling methods for proteomic profiling in living cells: An update Analysis of Proteins. (2020) doi:10.1002/wdev272.
63. Dundas, C. M., Demonte, D. & Park, S. Streptavidin-biotin technology: Improvements and innovations in chemical and biological applications. *Appl Microbiol Biotechnol* **97**, 9343–9353 (2013).
64. Qin, W., Cho, K. F., Cavanagh, P. E. & Ting, A. Y. Deciphering molecular interactions by proximity labeling. *Nature Methods* vol. 18 133–143 Preprint at https://doi.org/10.1038/s41592-020-01010-5 (2021).
65. Branon, T. C. *et al.* Efficient proximity labeling in living cells and organisms with TurboID. *Nat Biotechnol* **36**, 880–898 (2018).
66. May, D. G., Scott, K. L., Campos, A. R. & Roux, K. J. Comparative Application of BioID and TurboID for Protein-Proximity Biotinylation. *Cells* **9**, (2020).
67. Kim, K. eun *et al.* Dynamic tracking and identification of tissue-specific secretory proteins in the circulation of live mice. *Nat Commun* **12**, (2021).

68. Schildge, S., Bohrer, C., Beck, K. & Schachtrup, C. Isolation and culture of mouse cortical astrocytes. *J Vis Exp* (2013) doi:10.3791/50079.
69. Güler, B. E., Krzysko, J. & Wolfrum, U. Isolation and culturing of primary mouse astrocytes for the analysis of focal adhesion dynamics. *STAR Protoc* **2**, (2021).
70. Eng, L. F. *Glial Fibrillary Acidic Protein (GFAP)" the Major Protein of Glial Intermediate Filaments in Differentiated Astrocytes*. *Journal of Neuroimmunology* vol. 8 (1985).
71. Huang, H., He, W., Tang, T. & Qiu, M. Immunological Markers for Central Nervous System Glia. *Neuroscience Bulletin* vol. 39 379–392 Preprint at https://doi.org/10.1007/s12264-022-00938-2 (2023).
72. Greif, K. F., Asabere, N., Lutz, G. J. & Gallo, G. Synaptotagmin-1 promotes the formation of axonal filopodia and branches along the developing axons of forebrain neurons. *Dev Neurobiol* **73**, 27–44 (2013).
73. Ilan, N. & Madri, J. A. PECAM-1: Old friend, new partners. *Current Opinion in Cell Biology* vol. 15 515–524 Preprint at https://doi.org/10.1016/S0955-0674(03)00100-5 (2003).
74. Peterson, G. L. *A Simplification of the Protein Assay Method of Lowryetal. Which Is More Generally Applicable*. *ANALYTICAL BIOCHEMISTRY* vol. 83 (1977).
75. Barczak, W., Suchorska, W., Rubiś, B. & Kulcenty, K. Universal Real-Time PCR-Based Assay for Lentiviral Titration. *Mol Biotechnol* **57**, 195–200 (2015).
76. Lee, Y., Messing, A., Su, M. & Brenner, M. GFAP promoter elements required for region-specific and astrocyte-specific expression. *Glia* **56**, 481–493 (2008).
77. Wu, B. Y., Liu, R. Y., So, K. L. & Yu, A. C. H. *Multi-Lipofection Efficiently Transfected Genes into Astrocytes in Primary Culture*. *Journal of Neuroscience Methods* vol. 102 www.elsevier.com/locate/jneumeth (2000).
78. Cibelli, A. *et al.* Generation and Characterization of Immortalized Mouse Cortical Astrocytes From Wildtype and Connexin43 Knockout Mice. *Front Cell Neurosci* **15**, (2021).
79. Sakuma, T., Barry, M. A. & Ikeda, Y. Lentiviral vectors: Basic to translational. *Biochemical Journal* vol. 443 603–618 Preprint at https://doi.org/10.1042/BJ20120146 (2012).
80. Andersen, C. R., Nielsen, L. S., Baer, A., Tolstrup, A. B. & Weilguny, D. Efficient expression from one CMV enhancer controlling two core promoters. *Mol Biotechnol* **48**, 128–137 (2011).

81. Alliot, F. & Pessac, B. Astrocytic cell clones derived from established cultures of 8-day postnatal mouse cerebella. *Brain Res* **306**, 283–291 (1984).
82. Foo, L. C. *et al.* Development of a method for the purification and culture of rodent astrocytes. *Neuron* **71**, 799–811 (2011).
83. Lange, S. C., Bak, L. K., Waagepetersen, H. S., Schousboe, A. & Norenberg, M. D. Primary cultures of astrocytes: Their value in understanding astrocytes in health and disease. *Neurochemical Research* vol. 37 2569–2588 Preprint at https://doi.org/10.1007/s11064-012-0868-0 (2012).
84. Górska, A. M. *et al.* Evaluation of cerebrospinal fluid (CSF) and interstitial fluid (ISF) mouse proteomes for the validation and description of Alzheimer's disease biomarkers. *J Neurosci Methods* **411**, (2024).
85. Kutner, R. H., Zhang, X. Y. & Reiser, J. Production, concentration and titration of pseudotyped HIV-1-based lentiviral vectors. *Nat Protoc* **4**, 495–505 (2009).
86. Lin, P. *et al.* Efficient Lentiviral Transduction of Human Mesenchymal Stem Cells That Preserves Proliferation and Differentiation Capabilities. *Stem Cells Transl Med* **1**, 886–897 (2012).
87. Hauber, I. *et al.* Improving lentiviral transduction of CD34+ hematopoietic stem and progenitor cells. *Hum Gene Ther Methods* **29**, 104–113 (2018).
88. Gibbs, R. A. *et al.* Genome sequence of the Brown Norway rat yields insights into mammalian evolution. *Nature* **428**, 493–521 (2004).
89. Rabouille, C. Pathways of Unconventional Protein Secretion. *Trends in Cell Biology* vol. 27 230–240 Preprint at https://doi.org/10.1016/j.tcb.2016.11.007 (2017).
90. Cho, K. F. *et al.* Proximity labeling in mammalian cells with TurboID and split-TurboID. *Nat Protoc* **15**, 3971–3999 (2020).
91. Banerjee-Basu, S. & Packer, A. SFARI Gene: an evolving database for the autism research community. *Dis Model Mech* **3**, 133–135 (2010).
92. Wu, Y., Li, X., Liu, J., Luo, X. J. & Yao, Y. G. SZDB2.0: an updated comprehensive resource for schizophrenia research. *Hum Genet* **139**, 1285–1297 (2020).
93. Savage, J. T., Ramirez, J., Risher, W. C., Irala, D. & Eroglu, C. SynBot: An open-source image analysis software for automated quantification of synapses. doi:10.1101/2023.06.26.546578.

7. Supplementary information

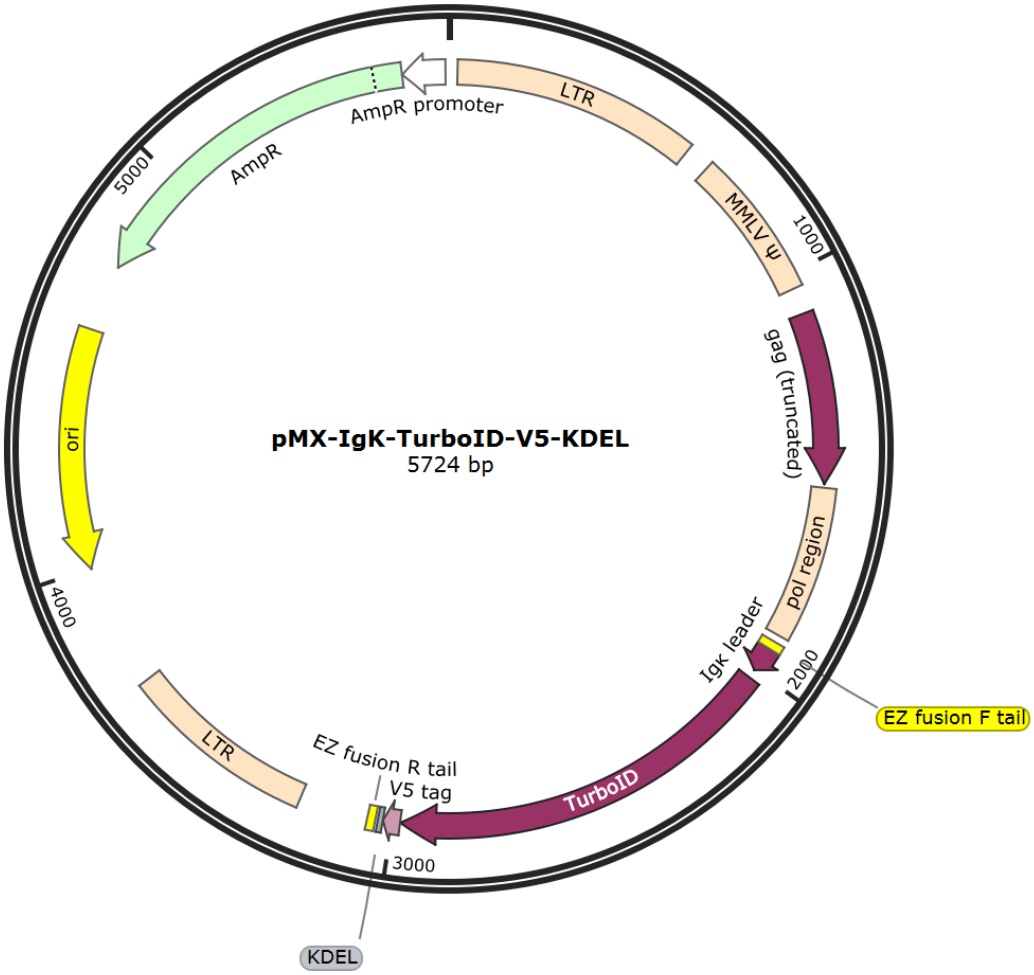

Figure S1 – pMX-IgK-TurboID-V5-KDEL plasmid map.

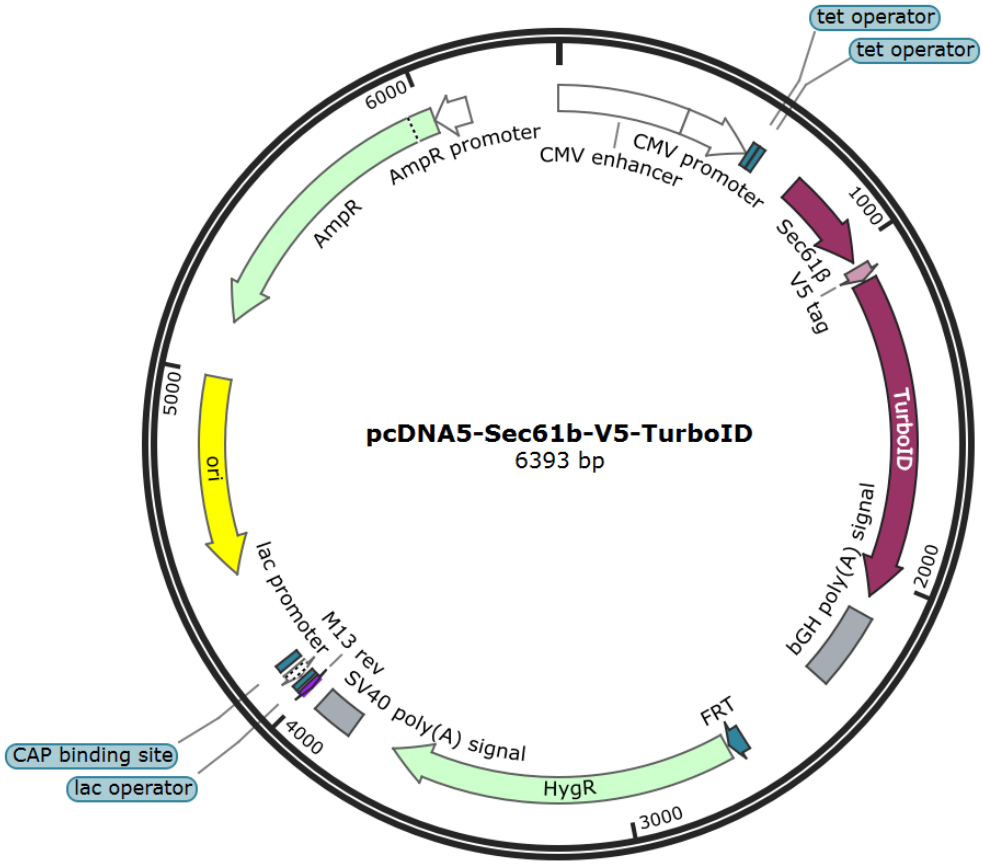

Figure S2 – pcDNA5-Sec61b-V5-TurboID plasmid map.

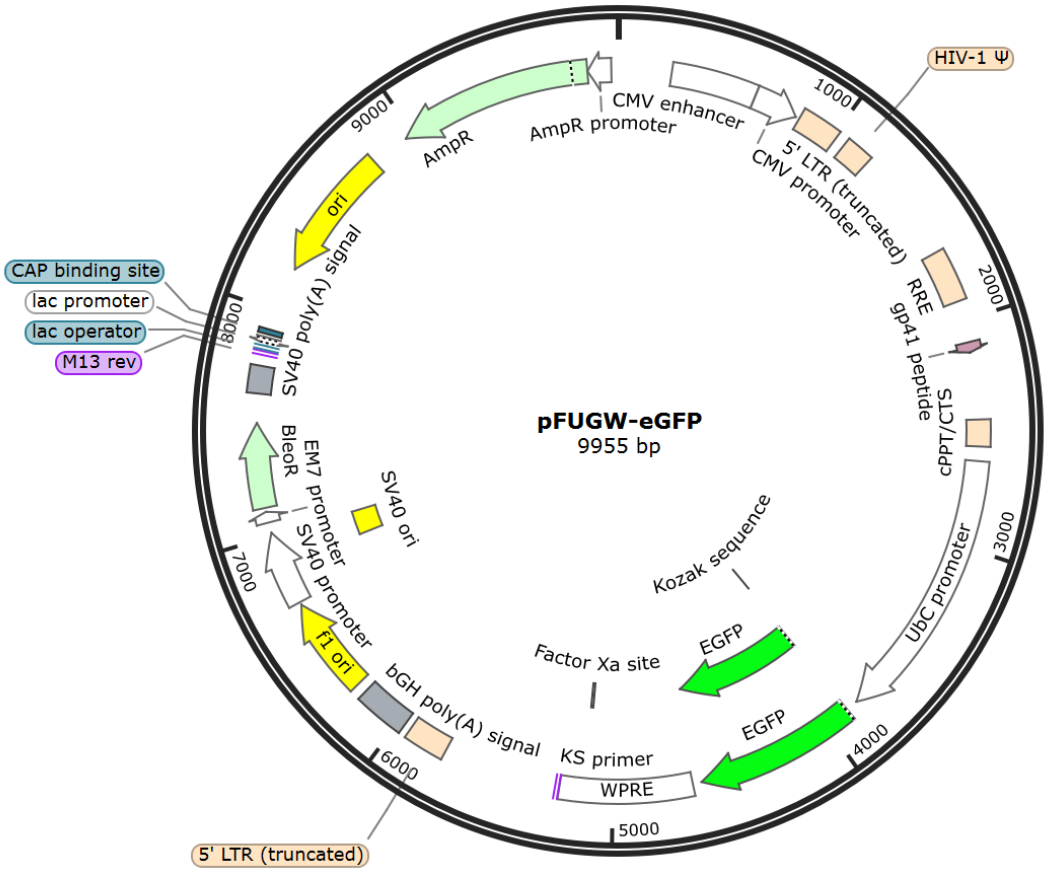

Figure S3 – pFUGW-eGFP plasmid map.

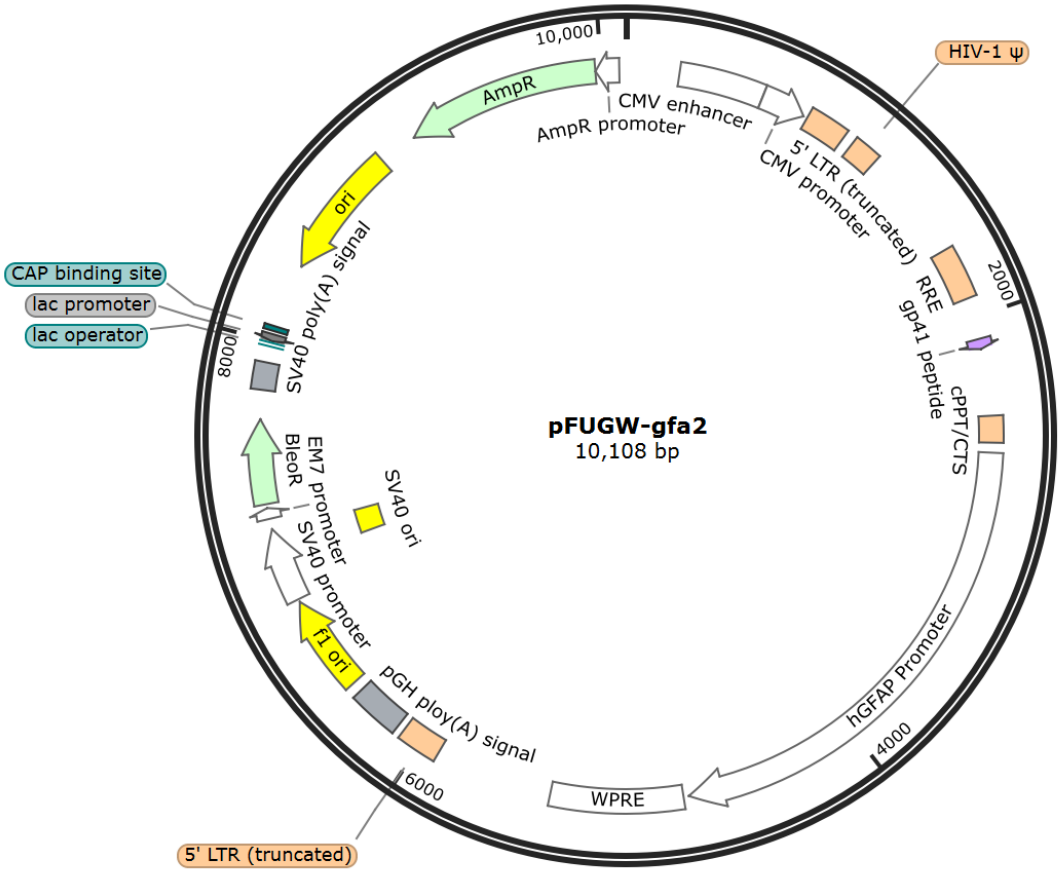

Figure S4 – pFUGW-gfa2 plasmid map.

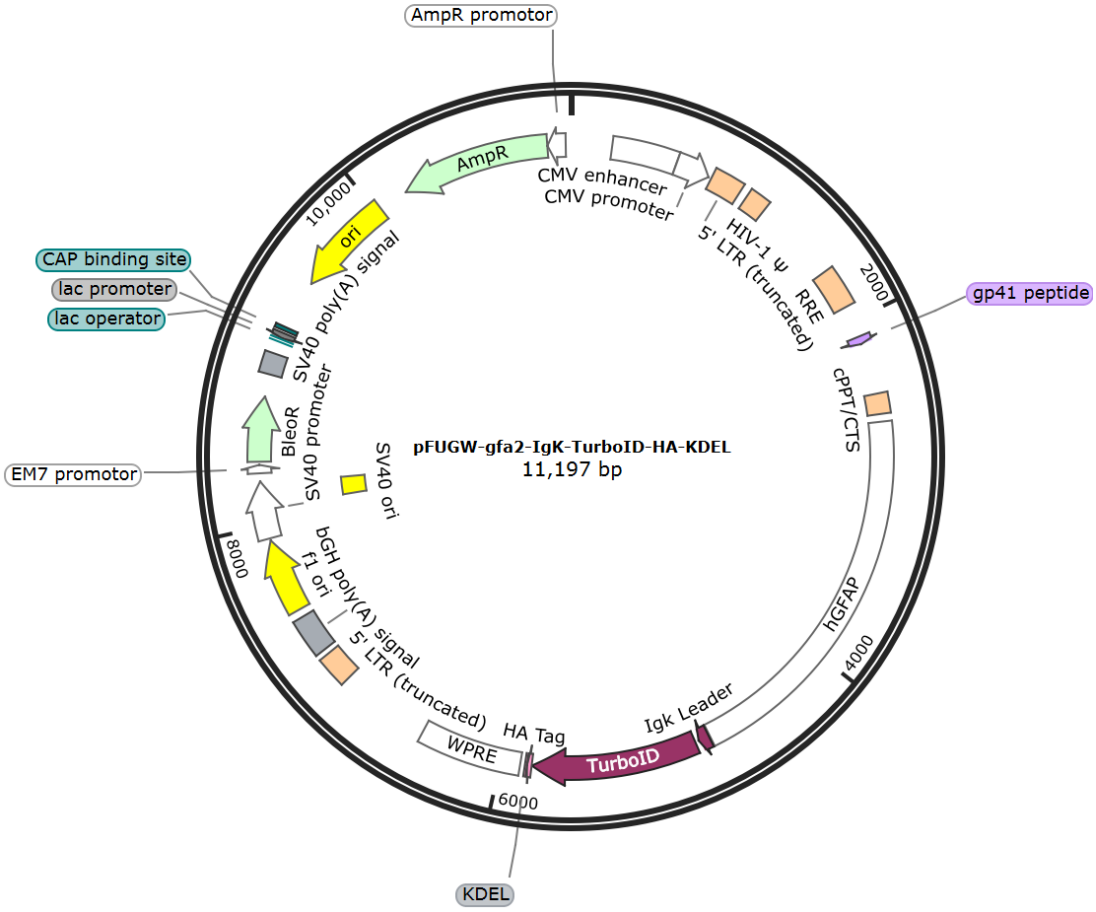

Figure S5 – pFUGW-gfa2-IgK-TurboID-HA-KDEL plasmid map.

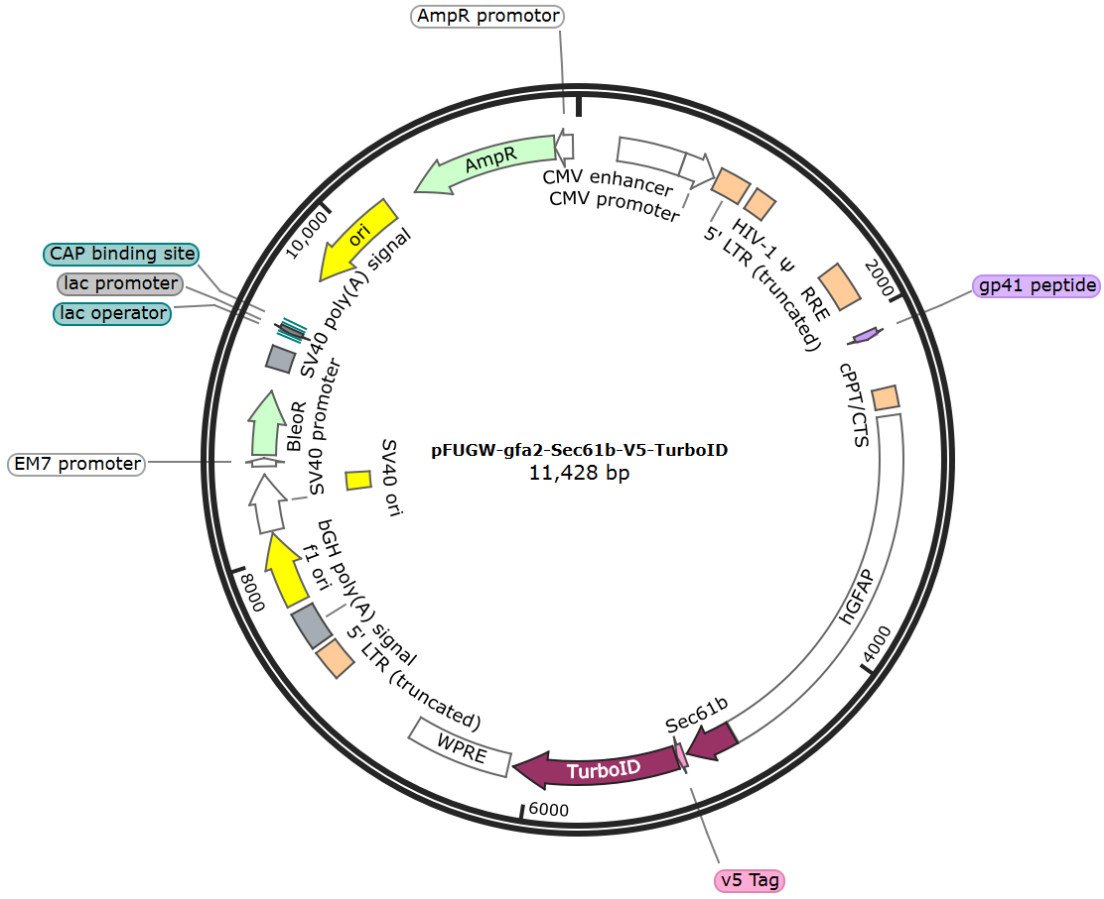

Figure S6 – pFUGW-gfa2-Sec61b-V5-TurboID plasmid map.

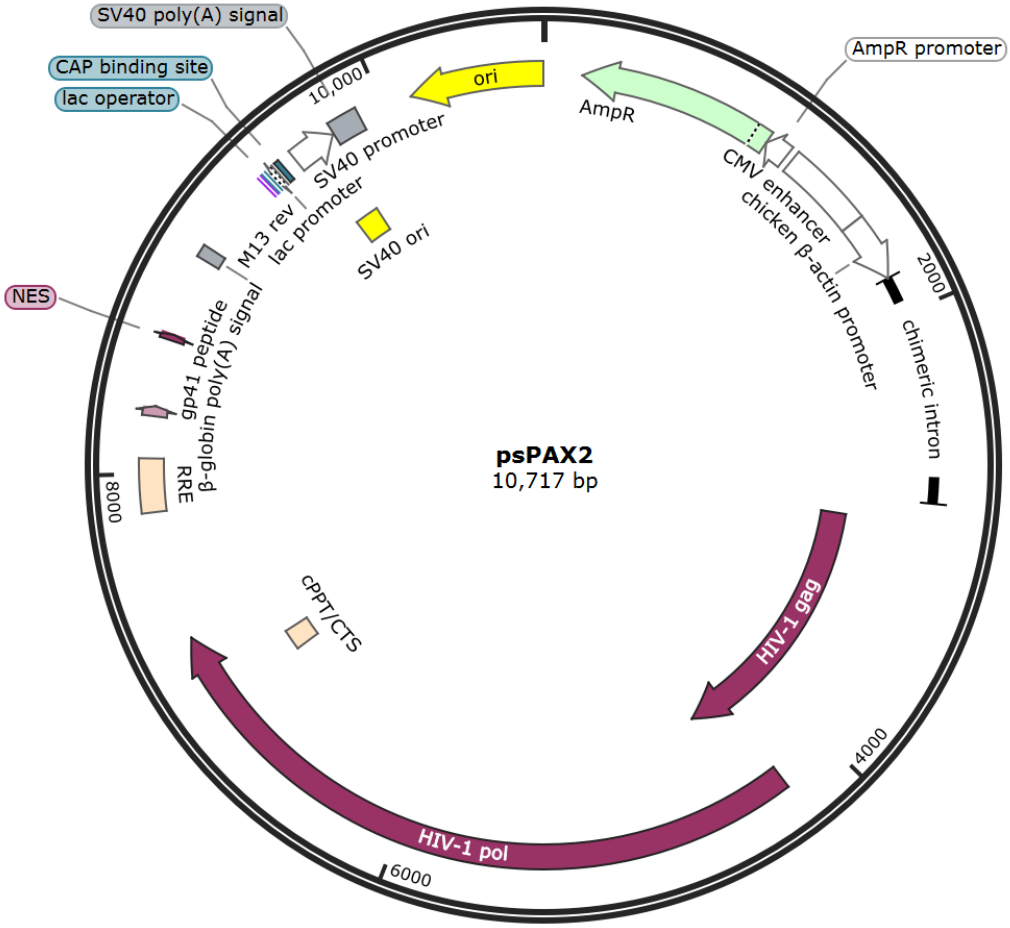

Figure S7 – psPAX2 plasmid map.

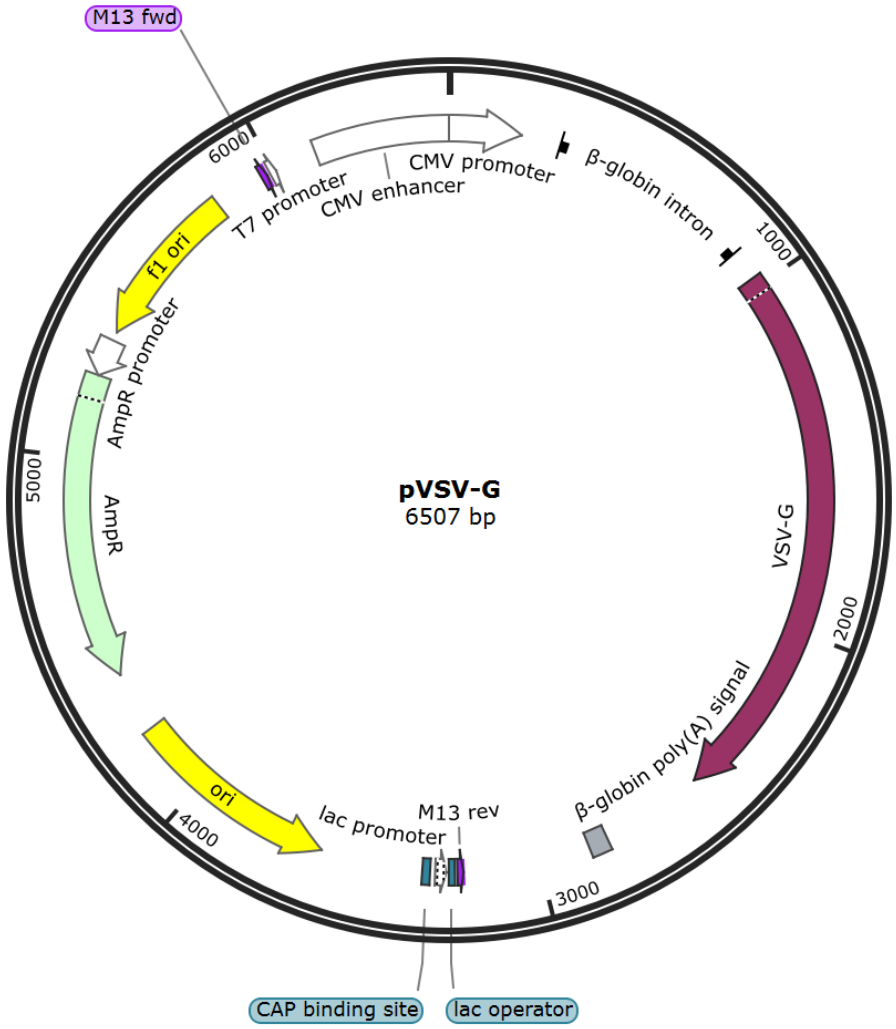

Figure S8 – pVSV-G plasmid map.

FACULDADE DE **MEDICINA**